Developing correction factors for weather's influence on the energy efficiency indicators of container ships using model-based machine learning

Godet, Amandine; Wallner, Lukas Jonathan Michael; Panagakos, George; Barfod, Michael Bruhn

Published in:
Ocean and Coastal Management

Link to article, DOI:
10.1016/j.ocecoaman.2024.107390

Publication date:
2024

Document Version
Publisher's PDF, also known as Version of record

Ocean and Coastal Management 258 (2024) 107390

Contents lists available at ScienceDirect

Ocean and Coastal Management

journal homepage: www.elsevier.com/locate/ocecoaman

Developing correction factors for weather's influence on the energy efficiency indicators of container ships using model-based machine learning

Amandine Godet, Lukas Jonathan Michael Wallner, George Panagakos, Michael Bruhn Barfod *

Department of Technology, Management and Economics, Technical University of Denmark, Akademivej 358, 2800 Kongens Lyngby, Denmark

ARTICLE INFO

Keywords:
Energy efficiency indicators
Fuel consumption
Weather effect
EEDI
Maritime policy

ABSTRACT

The International Maritime Organization employs technical and operational indicators to assess ship energy efficiency. Weather conditions significantly impact ship fuel consumption during voyages, necessitating the consideration of this influence in energy efficiency calculations. This study aims to design models for estimating the impact of weather components on fuel consumption and develop correction factors to cope with the weather effect on the fuel consumption of container ships for different sea states. Using model-based machine learning, the study analyzes noon reports and hindcasted weather data from two sister container ships. It quantifies weather-induced fuel consumption across various sea states, ranging from 2% to 20%, with an average of 7%–13% depending on the model used. Correction factors specific to each sea state are derived, and different approaches for their integration into energy efficiency indicators are proposed. This study advocates tailored weather correction factors for energy efficiency metrics tied to specific sea states, emphasizing the need for standardized weather impact assessments. Prior to any formal policy application, future work is needed to address the limitations of the present study and extend this approach to various ship types and sizes and different geographical regions.

1. Introduction

The imperative of decarbonization is one of the most significant challenges facing the maritime industry while sustaining the need for globalized transportation. The International Maritime Organization (IMO) set a revised Greenhouse Gas (GHG) reduction strategy in 2023 to achieve zero GHG emissions by or around 2050 (IMO, 2023). The IMO discussed and implemented different measures to achieve this reduction goal. Several of these measures target energy efficiency standards, namely the Energy Efficiency Design Index (EEDI), the Ship Energy Efficiency Management Plan (SEEMP), and the Carbon Intensity Indicator (CII). The EEDI, implemented in 2013, requires an increasing level of energy efficiency for new ships (Polakis et al., 2019), while the SEEMP and CII, respectively implemented in 2013 and 2023, relate to the operational efficiency. These regulations rely on energy efficiency indicators, which depend on many factors, including external factors beyond the operator's control (Panagakos et al., 2019).

Weather conditions is the most unpredictable among these external factors. A definition of the term 'weather' in the context of the present study is due right at the outset. Apart from navigation under icy conditions, which has structural implications for ship design, 'weather' is used in naval architecture and marine engineering to collectively denote those conditions that add to the calm-water resistance of a ship, thus, affecting the energy required for its propulsion. These conditions or 'weather components' are the waves (height and direction), the swells (height and direction), and the wind (direction and speed) (Bilgili, 2023). Note that the added resistance can be positive or negative depending on the direction of the weather components in relation to the bow of the vessel.

The effect of weather on energy requirements reflects directly on the 'energy efficiency' of the ship, another term that requires early clarification. In the context of waterborne transport, the term denotes the total energy required to produce one unit of transport work (expressed in nautical miles, hours of sailing, tonne-miles, etc.) under specific operational conditions (ship speed, draft, trim, etc.). All diverse sources of energy (chemical, electrical, wind, solar) enter the calculation of energy efficiency, which also depends on the energy saving devices installed onboard. For the purposes of the present study, the sample ships are propelled solely via chemical energy (fuel burned in marine internal combustion engines) and there is no modification in the energy saving devices installed during the study period. Furthermore, the different fuel qualities used have been transformed into Heavy Fuel Oil (HFO) equivalent quantities through the energy content or Lower Calorific Value (LCV) of the respective fuels. Under these conditions, 'energy efficiency' is equal to 'fuel consumption' (per unit of transport

* Corresponding author.
E-mail address: mbba@dtu.dk (M.B. Barfod).

https://doi.org/10.1016/j.ocecoaman.2024.107390
Received 3 April 2024; Received in revised form 26 August 2024; Accepted 15 September 2024
Available online 20 September 2024

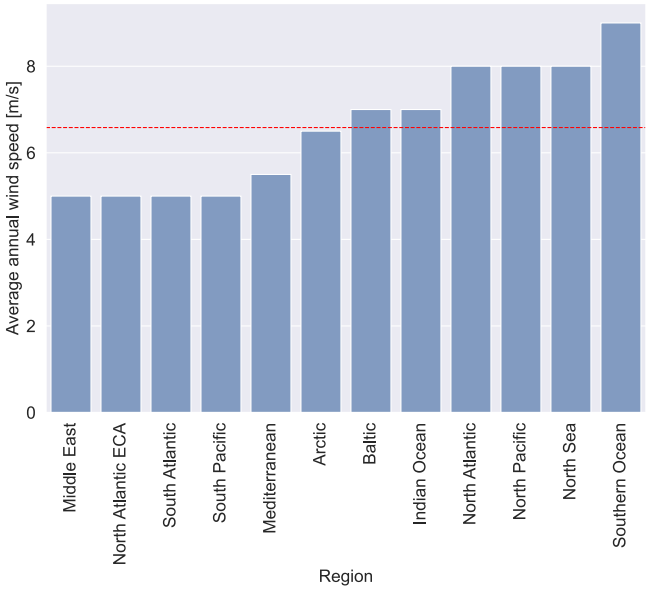

Fig. 1. Regional average wind speed. The red dashed line indicates the mean value. Own representation based on Rehmatulla et al. (2017).

work) multiplied by the constant LCV of HFO. Thus, the two terms are herewith used interchangeably.

The Third IMO GHG study 2014 (Smith et al., 2014) assumes that weather effects alone are responsible for approximately 15% of additional power on top of the theoretical calm-water propulsion requirements of ocean-going ships. The same weather correction factor is used in the Fourth IMO GHG study 2020 (Faber et al., 2020) for the different ship types and sizes examined. As illustrated in Fig. 1, weather conditions vary seasonally and regionally, affecting the energy efficiency of ships to a varying extent.

In turn, weather influences a ship's energy efficiency assessment when using operational indicators (e.g., for the CII), introducing biases and rendering these indicators problematic for benchmarking purposes. For instance, Panagakos et al. (2019) study different operational and external conditions (loading conditions, sea state, and wind direction) and conclude that the weather is the most uncontrollable of these conditions. As a result, the authors advocate for a specific approach that considers the weather's impact on operational and technical indicators intended for benchmarking purposes.

As the EEDI calculation uses calm weather conditions, the IMO introduced a weather correction factor f_w to account for the reduced efficiency in actual sea conditions (IMO, 2012a). f_w is either calculated as a function of ship capacity through a reference line or as a ratio of speeds in weather conditions corresponding to Beaufort (BF) scale 6[1] and in calm water under constant power. Nevertheless, the use of f_w is not mandatory and remains limited because it reflects a specific sea state irrespective of the conditions prevailing in the areas where the ship is expected to sail (IMO, 2009). The IMO also discussed the inclusion of weather correction factors in the calculation of CII, albeit without any decision so far (IMO, 2021a).

Ongoing discussions about weather correction factors for technical and operational indicators highlight the need to estimate the influence of weather on ship energy efficiency in different sea conditions to obtain tailored corrections of indicators. The following subsection reviews the literature on the impact of weather on energy efficiency indicators and fuel consumption.

[1] The Beaufort scale is an empirical measure that relates wind speed to observed conditions at sea or on land spreading from 0 (calm) to 12 (hurricane) (ISO, 2015).

1.1. Literature review

Energy efficiency indicators can be divided into two categories:

- Technical indicators (EEDI and Energy Efficiency Index for eXisting ships (EEXI)), which assess the efficiency of a ship (new and existing, respectively) at the design level, and
- Operational indicators (i.e., Annual Efficiency Ratio (AER) and Energy Efficiency Operational Index (EEOI), collectively named CII) which monitor actual efficiency performance at sea.

As an external factor influencing energy efficiency, the weather impacts these indicators.

Regarding EEDI, Bøckmann and Steen (2016) study the $\text{EEDI}_{weather}$, which is the EEDI corrected by the factor f_w. They show that the value of EEDI corrected for weather depends slightly on the calculation method, showing a barrier towards implementing a weather correction factor in a harmonized way. Differences in design efficiency can lead to even more significant disparities when considering the weather. For instance, Polakis et al. (2019) highlight that f_w typically spans between 0.8 and 0.95 for slow-speed ships (bulk carriers, tankers), which indicates the existence of substantial disparities in design efficiency expressed by the normal EEDI. Therefore, Lindstad et al. (2019) suggest adjustments to EEDI calculation during sea trial tests, including upward adjustments to actual sea conditions coupled with downward adjustments to calm water conditions, to take this weather influence into account in the definition of the EEDI calculations.

The indicators for operational energy efficiency assessment face challenges that must be addressed before they can be used for benchmarking ships. For instance, Wang et al. (2021) use seven examples to illustrate paradoxes of the CII, depending on whether the CII is calculated based on demand, supply, or distance for the transport work. Zhang et al. (2019) address the weakness of the EEOI in terms of transport work, raising the issue of having in the denominator the cargo onboard, which is considered sensitive commercial information by the ship operators. They propose an alternative metric, the Energy Efficiency Performance Indicator, with a proxy of the transport work based on semi-empirical analyses.

While several academic studies look at the impact of weather on EEDI, only a few analyze the effect of weather on operational indicators. Panagakos et al. (2019) study for different bulk carriers how the sea state and the wind direction influence various operational indicators, including EEOI and AER. They conclude that weather is the most uncontrollable of these factors, needing special treatment when using operational indicators for benchmarking purposes (Panagakos et al., 2019).

Therefore, special attention is given to the influence of weather on energy efficiency indicators. The remaining of this subsection reviews the research on estimating the impact of weather on fuel consumption as an essential determinant of energy efficiency.

Different methods exist to study and predict the influence of weather on fuel consumption. These methods are usually divided between data-driven methods (referred to as "black-box models", including machine learning) and deterministic methods, referred to as "white-box models", using test data (towing tank, wind tunnel), full-scale measurements, or Computational Fluid Dynamics (CFD). Additionally, hybrid methods combine data-driven and deterministic methods into "grey-box models". While Fan et al. (2022) provide a comprehensive review of ship fuel consumption prediction models, this section focuses on how these models deal with the weather influence.

Firstly, data-driven methods have recently shown growing research interest due to improved computing capabilities and big data processing potential. For example, Bocchetti et al. (2015) use multiple linear regressions to predict the fuel consumption on a specific voyage, taking into account operational conditions, including wind speed and direction (no wave), to assess the performance of the efficiency measures and operations. Wang et al. (2018) employ LASSO regression to predict fuel

consumption and include environmental factors (wind speed and direction, wave height and direction, swell height and direction). Hu et al. (2019) compare two techniques (Back-Propagation Neural Network and Gaussian Process Regression) regarding accuracy and computing time to predict fuel consumption, considering wind and current speed and direction and wave height and direction. Du et al. (2019) propose Artificial Neural Network (ANN) models to improve speed and trim optimization, adding the sea water temperature to the environmental parameters used by Hu et al. (2019).

Other data-driven models include a random forest regression model by Yan et al. (2020) for speed optimization, and they find that the current type has the most negligible impact on fuel consumption compared to wave and wind. Hu et al. (2021) find that waves have the most significant impact on the model, followed by wind and current when developing a fuel consumption prediction model. Megawati et al. (2023) propose a guide to develop ANN models for predicting ship fuel consumption while considering weather conditions. Kim et al. (2021) also use ANN, combined with a domain-knowledge-based method, to predict the fuel consumption of a container ship, with a focus on the draft to maximize efficiency. And Fan et al. (2024) evaluate different machine learning models for fuel prediction of a bulk carrier using onboard sensor and raise the issue of interpretability of such models. They conclude that the random forest and XGBOOST (based on decision trees) models best predict fuel consumption.

Secondly, semi-empirical methods are widely used to predict fuel consumption. Recently, Lang and Mao (2020) propose improvements to existing models for predicting speed loss in head waves. Vinayak et al. (2021) calculate the effect of weather (waves and wind) on vessel resistance for a tanker and a car carrier on different routes. Kim et al. (2023) provide a power performance prediction model, the Maritime Transport Environmental Assessment Model (MariTEAM), using Automatic Identification System (AIS) data, ship information, and weather hindcast data. Tadros et al. (2022) study the propeller performance for different sea states by modeling the added resistance in actual weather conditions. Finally, Vinayak et al. (2021) simulate the effect of wave and wind for a specific route, using historical weather data of 27 years and looking at the seasonal influence to optimize the route.

Thirdly, Computational Fluid Dynamics (CFD) simulations are also gaining traction due to improvements in software and increased computational power. For example, Grlj et al. (2023) determines wind load coefficients and air resistance of a container ship and the effect of trim, which is found to be negligible on wind resistance.

While all these methods can predict ship fuel consumption considering environmental factors (wind, waves, current, temperature, fouling, etc.) and different operational factors (speed, draft, trim, etc.), they do not estimate the contribution of these factors to fuel consumption. Few studies provide such an estimate, such as Meng et al. (2016), who quantify the contribution of bad weather to fuel consumption for four container ships in different wave directions. Kim et al. (2017) predict speed loss and sea margin for different speeds for a specific sea state (Beaufort 6) and the same heading. Bialystocki and Konovessis (2016) study the effect of varying sea states on the fuel consumption of a car carrier, based on noon reports. And Bilgili (2023) determines the weights of external conditions (waves and wind) on nine oil tankers' resistance using ANN.

Nevertheless, there is a gap in the literature as none of these studies estimate the effect of these environmental factors on the energy efficiency indicators and their underlying implications on policy. Tran (2021) who evaluates the interaction between weather conditions and the EEOI constitutes the only exception. However, his analysis is based on a simulation application. Therefore, although sea conditions significantly impact energy efficiency indicators, weakening their benchmarking capacity, insufficient research has been conducted to estimate how weather affects these indicators using actual operational ship data. The present study addresses this gap.

Table 1
Ship particulars.

Capacity	8112 TEU
Deadweight at scantling draft	114,210 tons
Displacement at design draft	119,567 m^3
Length between perpendiculars	318 m
Breadth	43.2 m
Design draft	13 m
Main engine maximum continuous rating	61,776 kW

1.2. Aims and contributions

Considering the importance of weather in ship energy efficiency assessment and the lack of estimates in existing literature, this study aims to:

1. estimate the influence of weather components on fuel consumption
2. develop factors to correct the energy efficiency indicators for the influence of weather

The analysis relies on model-based machine-learning techniques, including linear and polynomial regressions and a grey-box model using fundamentals of ship hydrodynamics. The well-known advantages of machine-learning are, thus, enhanced with theoretical knowledge from the area of ship resistance and propulsion. In addition, the parallel examination of different models enables the direct comparison of their performance. The models learn from two years of noon reports of two sister container ships. Comparing their performance allows for selecting the best models and estimating the impact of weather components. Weather correction factors for different sea states are then developed and discussed, along with their policy implications.

The rest of this study is structured as follows: Section 2 presents the data sources and variables, which are further implemented in the models described in Section 3. Section 4 describes the resulting weather estimates and the definition of correction factors. Section 5 discusses the policy implications of these correction factors and addresses the limitations of the study. Finally, Section 6 concludes.

2. Data

The analysis relies on actual data, consisting of noon reports (daily reports from the ship officers), hindcast weather data, and technical characteristics from model tests provided by a globally leading container ship operator for two sister container ships sailing in 2018 and 2019. Table 1 details the ship particulars, and Fig. 2 illustrates the routes undertaken by the two ships.

2.1. Data selection

The inputs for the models, further described in Section 3, are:

- Operational variables: speed through water, average draft
- Ship variables: main dimensions, efficiency coefficients, resistance coefficients
- Weather variables: wave height and direction, swell height and direction, wind speed and direction

The prediction variable of all models is the ship's main engine fuel consumption. The selection and description of the independent variables (predictors) are presented below:

- Speed is available as speed through water and speed over ground in the noon reports. As ocean and tidal currents influence the speed over ground (Perera and Mo, 2018), the analysis considers only speed through water, which is independent of current influences.

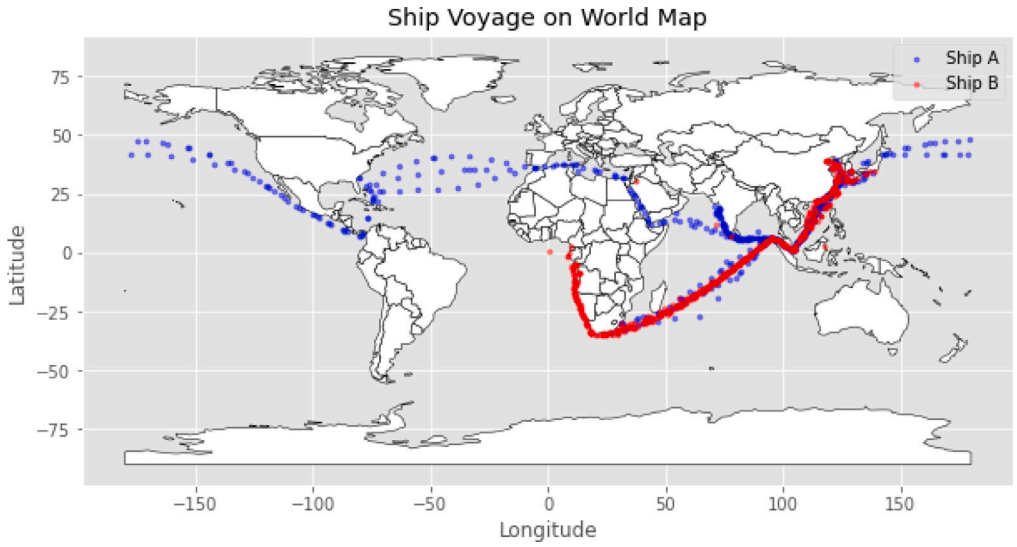

Fig. 2. Ships voyages.

Table 2
Number of reports.

	Raw number of reports	Number of sea reports (excluding port reports, anchorage, and channel passages)	Number of sea reports after filtering (missing data, unrealistic values)	Time period
Ship A	744	574	555	24 months
Ship B	663	527	494	24 months
Total	1407	1101	1049	

- The average draft is the mean of the fore and aft drafts, as reported in the noon reports.
- The weather variables cover wave and swell heights, wind speed, and the related directions (relative to the bow). These elements come from hindcast weather data (historical modeled data) reported every four hours and daily averaged to match the noon report.
  - Waves, also called wind waves, are distinguished from swells. Wind waves are "formed due to the direct action of local winds", while swells are "wind waves that have traveled out of the generating area" (Toffoli and Bitner-Gregersen, 2017).
  - Swells typically have longer periods and smaller heights than wind waves (Toffoli and Bitner-Gregersen, 2017).
  - The apparent wind speed and direction are available in the hindcast weather data.

In addition, ship variables account for different efficiency coefficients (e.g., hull efficiency) and resistance coefficients, as further detailed in Section 3 and Table 3. These variables are obtained from the company's ship class model tests, including the open water characteristics of the propeller model, the resistance test results, and the full-scale resistance prediction.

Other variables influence fuel consumption, such as trim, hull and propeller fouling, water depth, water salinity, and water temperature (Berthelsen and Nielsen, 2021). Apart from water salinity and temperature, these factors are not related to weather and fall outside the scope of the study. Moreover, trim and hull/propeller fouling are controllable by the ship operator, who should be accountable for the relevant effect on energy efficiency indicators anyway. No data on water depth, salinity and temperature was provided.

2.2. Data description

The data set provided by the container ship operator contains all noon reports generated manually by the officers onboard two sister container ships during 2018 and 2019. Reports with missing data for the selected variables and data with physically unrealistic values (speed over 30 knots, ship sailing at zero main engine power) are excluded to ensure data quality and consistency. Additionally, we keep only noon reports where the ship is sailing in the open sea, called 'sea reports,' where the weather conditions influence the ship's energy efficiency the most, thus excluding port stays, anchorage, and canal passages. Table 2 summarizes the number of noon reports used in the analysis before and after filtering.

The noon reports provide fuel consumption over the report duration, with separate figures for different fuel types, i.e., low- and high-sulfur heavy fuel oil and low- and high-sulfur diesel oil. The aggregate fuel consumption is calculated as the equivalent high-sulfur heavy fuel oil, weighting the different fuels by their lower calorific values. Note that the data reflects fuels used before the 1st January 2020, when the IMO rule limiting the sulfur content of marine fuels came into force (IMO, 2019).

It can be easily proven that the true wind speed V_{WT} can be calculated based on the ship's speed V, the apparent wind speed V_{WR}, and the apparent wind direction β_{aw} through:

$$V_{WT} = \sqrt{V^2 + V_{WR}^2 - (2 \cdot V \cdot V_{WR} \cdot \cos \beta_{aw})} \quad (1)$$

The wave, swell, and wind directions are reported on a 0° to 360° scale relative to the bow. Assuming that the ship responses to weather conditions are symmetrical (as in Taskar et al. (2021)), the scale is adjusted to 0° to 180°. Furthermore, for each weather component, categories are created for each range of directions, using dummy variables: 0° to 60° for the bow, 60° to 120° for the beam, and 120° to 180° for the stern. This categorization follows Bialystocki and Konovessis (2016),

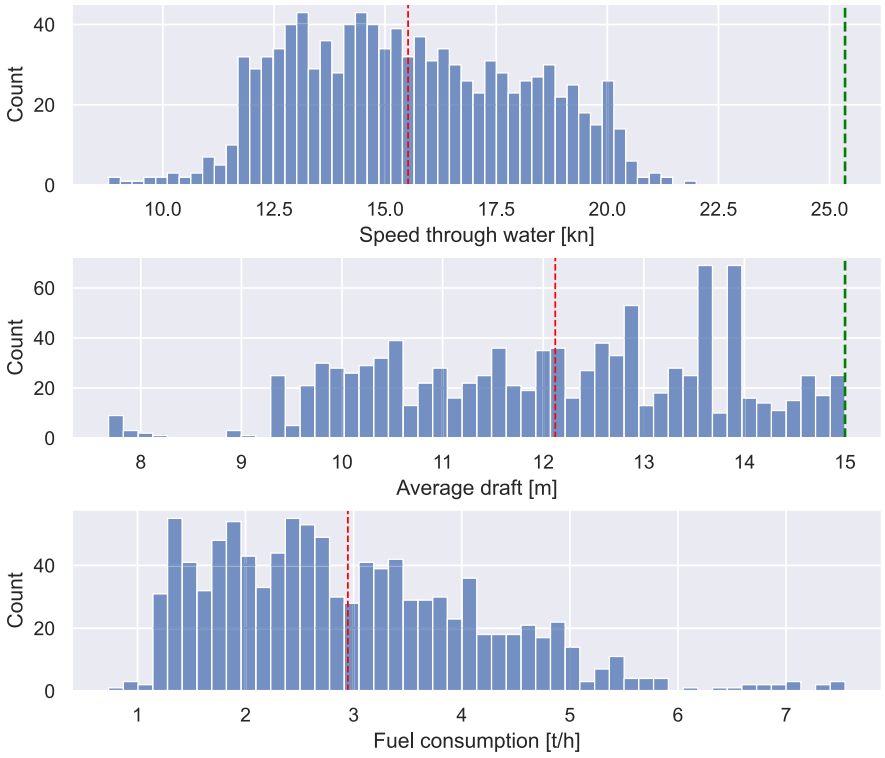

Fig. 3. Histograms of speed, draft, and fuel consumption. The red dashed lines represent the mean value, and the green dashed lines represent the design speed and the scantling draft.

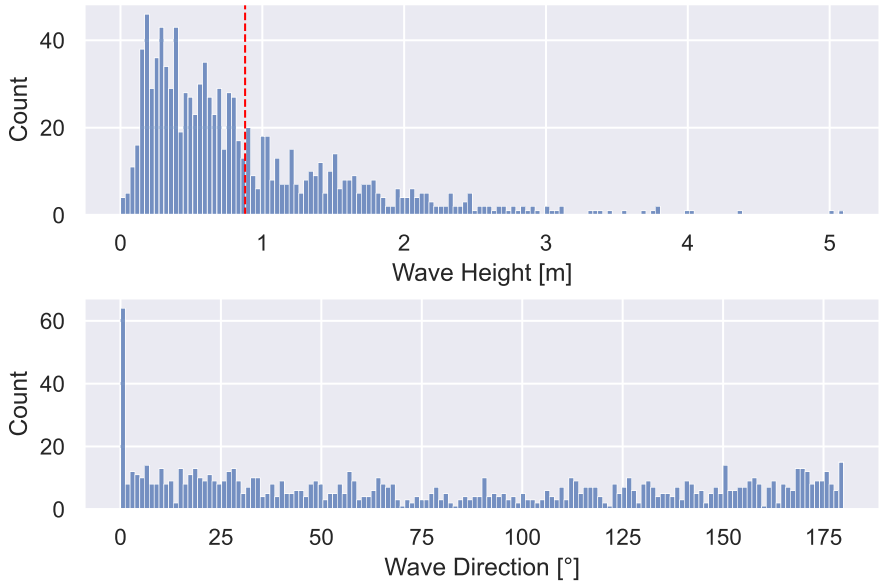

Fig. 4. Histograms of wave height and direction relative to the bow. The red dashed line represents the mean value.

who stated that the impact of the wind on a ship's hull is similar within the ranges 0° to 60°, 60° to 120°, and 120° to 180°. Lastly, sea states, spreading from 0 (calm) to 12 (hurricane), are defined based on the wind speed following the Beaufort (BF) scale (ISO, 2015).

Fig. 3 shows speed, draft, and fuel consumption histograms, Fig. 4 presents the histograms of wave height/direction and Fig. 5 of swell height/direction.

The mean wave height is 0.9 m, and the mean swell height is 1.5 m. In respectively 44% and 40% of the data points, the ship encounters head waves and swells. This high proportion of waves and swells coming on the bow is due to the method used by the company averaging hindcast weather observations (every four hours) to noon report level (24 h). Indeed, the wave/swell/wind energy is calculated for each weather observation. Then, the wave/swell/wind direction of the observation with the maximum energy component is used for the entire noon report.

Figs. 6 and 7, respectively, show the histograms of apparent wind speed/direction and true wind speed/direction. The mean apparent

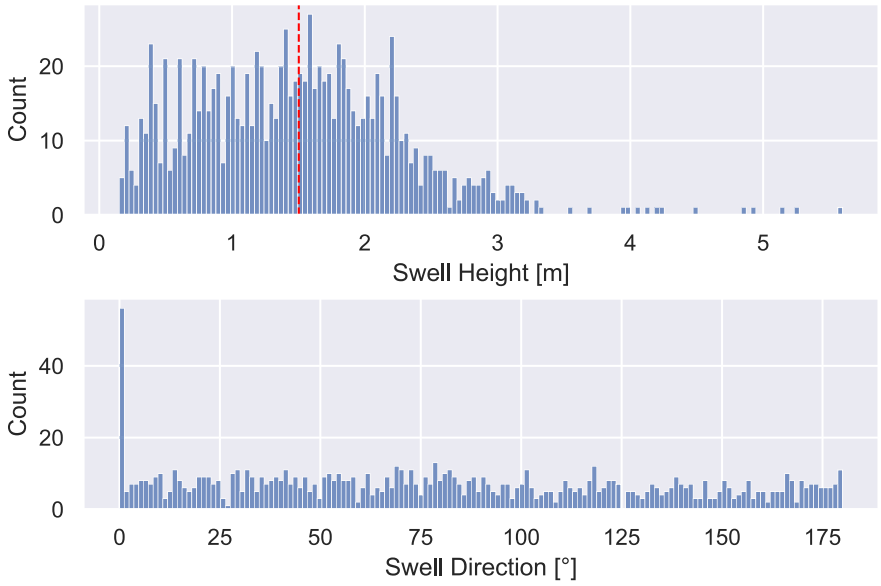

Fig. 5. Histograms of swell height and direction relative to the bow. The red dashed line represents the mean value.

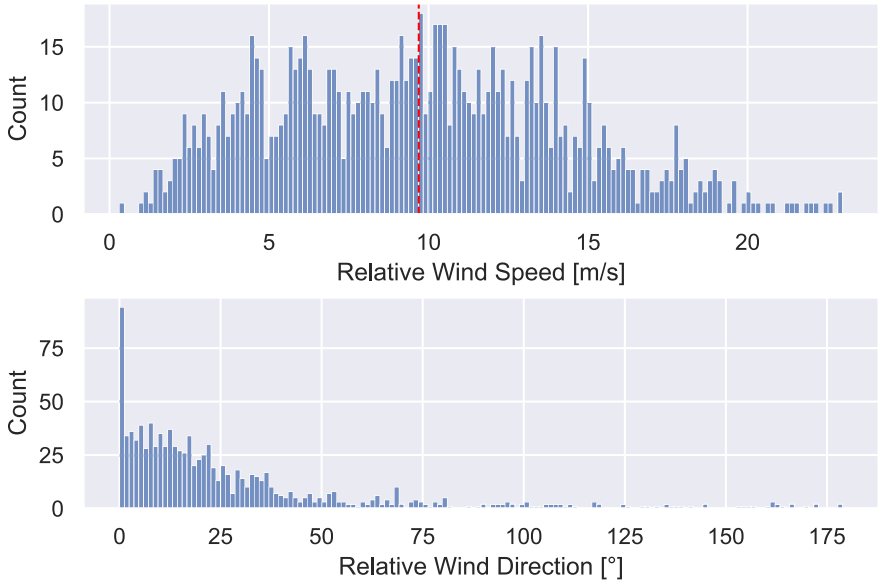

Fig. 6. Histograms for apparent wind speed and apparent wind direction. The red dashed line represents the mean value.

wind speed is 9.7 m/s. The mean true wind speed is 5.8 m/s, corresponding to Beaufort (BF) 4.[2]

Fig. 8 shows the distribution of the sea states according to the Beaufort scale, as calculated based on the true wind speed.

Table 3 summarizes the variables used in the models, further described in Section 3. Fig. 9 shows the Pearson correlation matrix of the different variables. Fuel consumption is highly correlated with ship speed (0.84), followed by the apparent wind speed (0.39). The relative wave direction shows a correlation of 0.54 with the apparent wind direction, expected as it is the wind that forms waves, and a correlation of 0.52 with the relative swell direction.

[2] The average of BF 4 differs from the average sea state presented in Table 3, as the latter is calculated based on the discrete sea state figures.

3. Methods

The estimation of the influence of weather on fuel consumption and energy efficiency requires interpretable models combining multiple explanatory variables. Model-based machine learning, or probabilistic machine learning, enables customized models individually designed for each particular use case (Bishop, 2013). Model-based machine learning relies on a Bayesian approach, which treats model parameters as random variables and expresses their uncertainty using probability distributions. The approach incorporates prior knowledge about parameters and updates it with observed data, resulting in posterior distributions. The following subsections describe the different models (linear regression, polynomial regression, and a grey-box model) using this Bayesian approach of model-based machine learning to estimate the influence of weather on fuel consumption. Two versions of the linear and polynomial regressions are formed, i.e., with and without

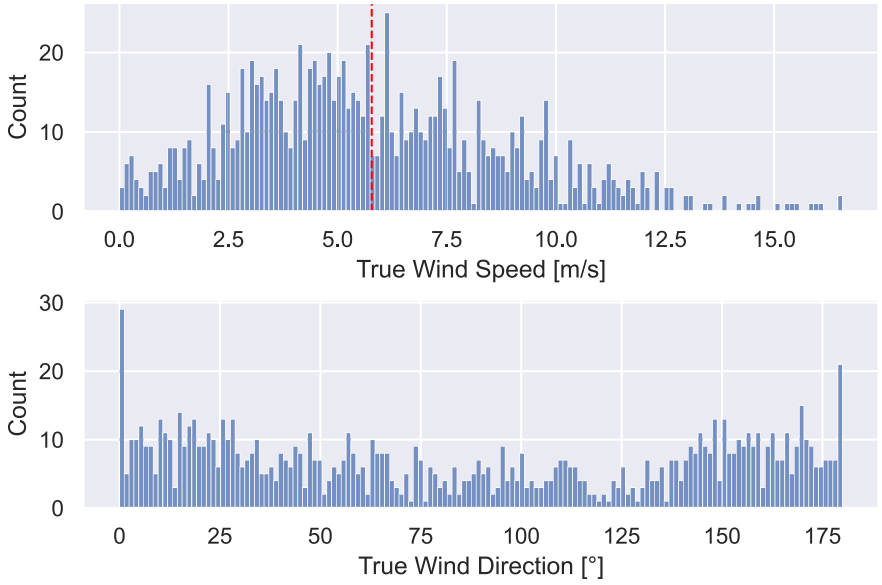

Fig. 7. Histograms for true wind speed and true wind direction. The red dashed line represents the mean value.

Table 3
Summary of variables.

Variable	Unit	Data source	Mean value	Range value
Output variable				
Hourly fuel consumption y	ton/h	Noon report	2.9	[0.7, 7.5]
Operational variables				
Speed through water V	kn	Noon report	15.5	[8.8, 22.0]
Average draft T	m	Noon report	12.1	[7.7, 15.0]
Weather variables				
Wave height	m	Hindcast weather	0.9	[0.0, 5.1]
Relative wave direction	°	Hindcast weather		[0, 180]
Swell height	m	Hindcast weather	1.5	[0.2, 5.6]
Relative swell direction	°	Hindcast weather		[0, 180]
Relative wind speed	m/s	Hindcast weather	9.7	[0.3, 23.0]
Relative wind direction	°	Hindcast weather		[0, 180]
True wind speed	m/s	Calculation	5.8	[0.0, 16.6]
True wind direction	°	Calculation		[0, 180]
Sea state (on Beaufort scale)	/	Calculation	3	[0, 7]
Dummy variables for weather				
Wave - Bow	/	Based on direction		{0, 1}
Wave - Beam	/	Based on direction		{0, 1}
Wave - Stern	/	Based on direction		{0, 1}
Swell - Bow	/	Based on direction		{0, 1}
Swell - Beam	/	Based on direction		{0, 1}
Swell - Stern	/	Based on direction		{0, 1}
Wind - Bow	/	Based on direction		{0, 1}
Wind - Beam	/	Based on direction		{0, 1}
Wind - Stern	/	Based on direction		{0, 1}
Resistance coefficients and efficiencies				
Air resistance coefficient C_{AA}	/	Model tests	−0.6	[−0.8, 0.9]
Frictional resistance coefficient C_F	/	Model tests	$1.4 \cdot 10^3$	
Hull efficiency η_H	/	Model tests	1.15	
Rotative efficiency η_R	/	Model tests	0.99	
Open-water efficiency η_O	/	Model tests	0.67	
Shaft efficiency η_S	/	Model tests	0.77	

directions of the weather components. Following model evaluation, only the directional versions are used for estimating the weather impact on fuel consumption. Correction factors on the energy efficiency indicators are calculated only for the best performing polynomial and grey-box models. Fig. 10 graphically depicts this flow chart.

3.1. Linear model

The first model is a linear regression model, including the weather parameters (wind, wave, and swell) without their directions. Despite the non-linear relation between some variables (e.g., between fuel consumption and ship or wind speeds), this model serves as the baseline for the performance evaluation of the different models. The linear model uses the field knowledge to constrain the parameter prior distributions. Unless stated otherwise, all parameters in the models have their standard deviation σ initialized to the default value of one. For the linear model without direction, prior knowledge leads to the following distributions:

- The fuel consumption y is assumed to be zero if all explanatory variables are zero, i.e., the ship is not in operation. Thus, the

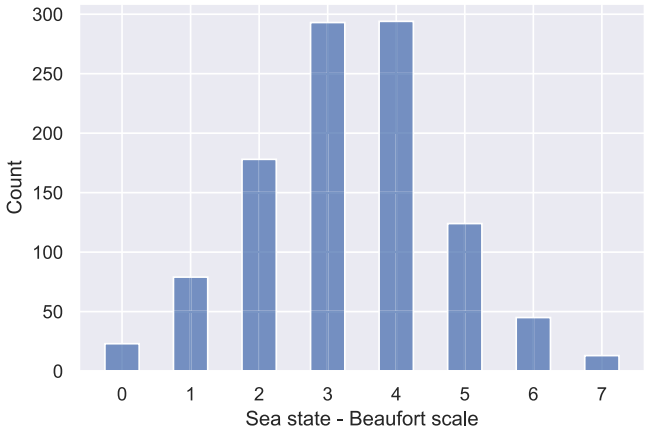

Fig. 8. Histogram of the sea state, according to the Beaufort scale.

intercept β_0 is an unconstrained normal distribution $\mathcal{N}$ with a zero mean: $\beta_0 \sim \mathcal{N}(0, 1)$.

- Ship speed is expected to strongly correlate with fuel consumption, as higher speeds generally lead to increased engine power. Thus, the coefficient β_{Speed} is modeled using a truncated normal distribution with a lower bound (a) of 0: $\beta_{Speed} \sim \mathcal{N}(0, 1, a = 0)$.
- An increase in draft leads to a greater wetted surface area, resulting in higher calm-water resistance and fuel consumption. Therefore, the respective coefficient β_{Draft} is modeled analogously to the others: $\beta_{Draft} \sim \mathcal{N}(0, 1, a = 0)$.
- While wind on the stern can decrease the fuel consumption (Perera and Mo, 2018), most data points reflect headwind. Therefore, the coefficient β_{Wind} is expected to be positive and modeled as a truncated normal distribution with a lower bound of 0: $\beta_{Wind} \sim \mathcal{N}(0, 1, a = 0)$.
- Since an increase in wave and swell heights increases the fuel consumption, their coefficients ($\beta_{Wave}, \beta_{Swell}$) are also modeled using a truncated normal distribution with a lower bound of zero: $\beta_{Wave}, \beta_{Swell} \sim \mathcal{N}(0, 1, a = 0)$.
- The fuel consumption is modeled as a linear combination of the previously introduced parameters. Its mean μ is shown below, where X are the explanatory variables, and the corresponding β coefficients follow the prior distributions previously mentioned. Since the fuel consumption y can never be negative, it is modeled using a truncated normal distribution with a lower bound of zero. The prior distribution for the standard deviation σ is chosen as a standard half-normal distribution, accounting for the non-negativity of σ.

$$\mu = \beta_0 + \beta_{Speed} \cdot X_{Speed} + \beta_{Draft} \cdot X_{Draft} + \beta_{Wind} \cdot X_{Wind} + \beta_{Wave} \cdot X_{Wave} + \beta_{Swell} \cdot X_{Swell}$$
$$\sigma \sim \mathcal{N}(0, 1, a = 0)$$
$$y \sim \mathcal{N}(\mu, \sigma, a = 0)$$

The next step is to build upon the previous model by adding directions to the weather parameters. The impact of cross-wind, cross-waves, and cross-swell is complex to quantify (Majidian and Azarsina, 2019). Therefore, the coefficients $\beta_{Wind\,Beam}$, $\beta_{Waves\,Beam}$, and $\beta_{Swell\,Beam}$ are modeled using an unbounded normal distribution. The negative relation between wind, waves, and swell on the stern and fuel consumption, as described by Perera and Mo (2018), is reflected by the coefficients $\beta_{Wind\,Stern}$, $\beta_{Waves\,Stern}$, and $\beta_{Swell\,Stern}$, modeled by a truncated normal distribution with an upper bound (b) of zero. The specifications of the probabilistic model are:

$$\beta_0, \beta_{Wind\,Beam}, \beta_{Wave\,Beam}, \beta_{Swell\,Beam} \sim \mathcal{N}(0, 1)$$
$$\beta_{Speed}, \beta_{Draft}, \beta_{Wind\,Bow}, \beta_{Wave\,Bow}, \beta_{Swell\,Bow} \sim \mathcal{N}(0, 1, a = 0)$$
$$\beta_{Wind\,Stern}, \beta_{Waves\,Stern}, \beta_{Swell\,Stern} \sim \mathcal{N}(0, 1, b = 0)$$
$$\mu = \beta_0 + \beta_{Speed} \cdot X_{Speed} + \beta_{Draft} \cdot X_{Draft} + \beta_{Wind\,Bow} \cdot X_{Wind\,Bow} + \beta_{Wind\,Beam} \cdot X_{Wind\,Beam} + \beta_{Wind\,Stern} \cdot X_{Wind\,Stern} + \beta_{Wave\,Bow} \cdot X_{Wave\,Bow} + \beta_{Wave\,Beam} \cdot X_{Wave\,Beam} + \beta_{Wave\,Stern} \cdot X_{Wave\,Stern} + \beta_{Swell\,Bow} \cdot X_{Swell\,Bow} + \beta_{Swell\,Beam} \cdot X_{Swell\,Beam} + \beta_{Swell\,Stern} \cdot X_{Swell\,Stern}$$
$$\sigma \sim \mathcal{N}(0, 1, a = 0)$$
$$y \sim \mathcal{N}(\mu, \sigma, a = 0)$$

3.2. Polynomial model

The polynomial regression model expands upon the linear model by including polynomials of the explanatory variables, fitting data with a non-linear curve, which allows the use of more prior knowledge (James et al., 2023). For instance, as further developed in Section 3.3, the relation between fuel consumption and speed is cubic, and Eqs. (7) and (8) show a squared relation between the fuel consumption on the one hand and the wind speed and wave height on the other. A similar relation is also assumed for the swell height. Knowing the exact exponents of the variables simplifies the polynomial model. Therefore, including only the identified exponents can avoid over-complexification. The model, without directions, is then:

$$\beta_0 \sim \mathcal{N}(0, 1)$$
$$\beta_{Speed}, \beta_{Draft}, \beta_{Wind}, \beta_{Wave}, \beta_{Swell} \sim \mathcal{N}(0, 1, a = 0)$$
$$\mu = \beta_0 + \beta_{Speed} \cdot X_{Speed}^3 + \beta_{Draft} \cdot X_{Draft} + \beta_{Wind} \cdot X_{Wind}^2 + \beta_{Wave} \cdot X_{Wave}^2 + \beta_{Swell} \cdot X_{Swell}^2$$
$$\sigma \sim \mathcal{N}(0, 1, a = 0)$$
$$y \sim \mathcal{N}(\mu, \sigma, a = 0)$$

The polynomial regression model with directions is also investigated, using the same distributions as for the linear model. The only difference lies in the μ term, as follows:

$$\mu = \beta_0 + \beta_{Speed} \cdot X_{Speed}^3 + \beta_{draft} \cdot X_{draft} + \beta_{Wind\,Bow} \cdot X_{Wind\,Bow}^2 + \beta_{Wind\,Beam} \cdot X_{Wind\,Beam}^2 + \beta_{Wind\,Stern} \cdot X_{Wind\,Stern}^2 + \beta_{Waves\,Bow} \cdot X_{Wave\,Bows}^2 + \beta_{Waves\,Beam} \cdot X_{Waves\,Beam}^2 + \beta_{Waves\,Stern} \cdot X_{Waves\,Stern}^2 + \beta_{Swell\,Bow} \cdot X_{Swell\,Bow}^2 + \beta_{Swell\,Beam} \cdot X_{Swell\,Beam}^2 + \beta_{Swell\,Stern} \cdot X_{Swell\,Stern}^2$$

3.3. Grey-box model

Lastly, a grey-box model directly reflects domain knowledge by tuning prior distributions with ship hydrodynamic fundamentals. According to Birk (2019), the brake power P_B, needed to propel the ship, depends on the total ship resistance R_T, the ship speed V, and several efficiency coefficients (hull efficiency η_H, relative rotative efficiency η_R, propeller efficiency in open water η_O, shafting efficiency η_S, gearing efficiency η_G), as illustrated in Fig. 11 following the ITTC terminology (ITTC, 2021).

$$P_B = \frac{R_T \cdot V}{\eta_H \cdot \eta_R \cdot \eta_O \cdot \eta_S \cdot \eta_G} \tag{2}$$

The total resistance R_T is the sum of the calm-water resistance and the added resistance due to weather conditions. The calm-water resistance is composed of the frictional resistance (friction between the hull and the water), the air resistance (from the ship's superstructure and hull above waterline), and the residual resistance (Birk, 2019). The residual resistance accounts for additional effects unrelated to weather conditions and, therefore, omitted here as their description and calculation are complex and left to specialized literature. Consequently, the total resistance R_T becomes the sum of frictional resistance R_F, the air resistance R_{AA}, the added wind resistance ΔR_{wind}, and the added

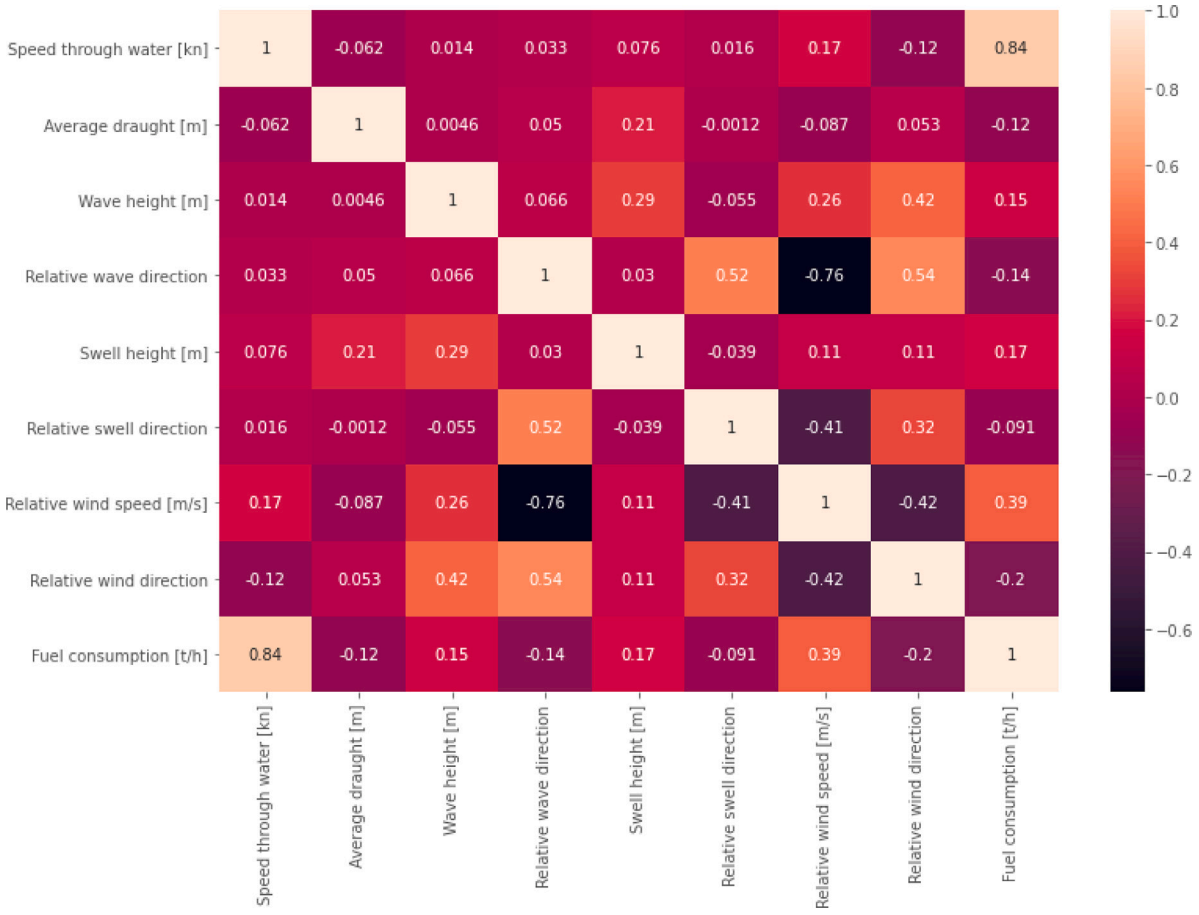

Fig. 9. Correlation matrix of the variables.

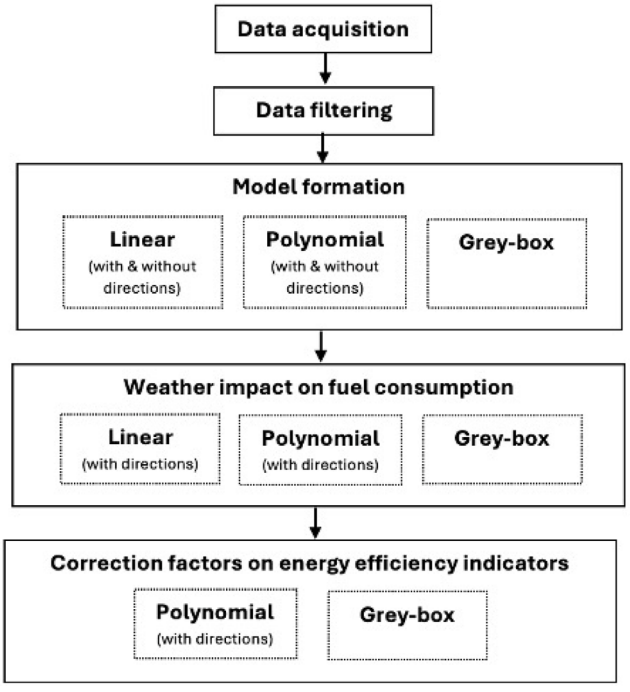

Fig. 10. Flow chart of the analysis performed.

wave resistance ΔR_{waves}. Therefore, the fuel consumption consists of the fuel consumption in calm water and the added fuel consumption due to weather conditions. The former mainly depends on the ship's speed and draft, while the latter depends on wind, waves, and swells.

Eq. (3) shows the formula for the frictional resistance:

$$R_F = \frac{1}{2} \cdot C_F \cdot \rho \cdot S \cdot V^2 \tag{3}$$

where C_F is the frictional resistance coefficient, ρ the water mass density, S the area of wetted surface, and V the ship's speed. The area of wetted surface S is calculated based on Mumford's formula (Birk, 2019):

$$S = 1.025 \cdot L_{pp} \cdot (C_B \cdot B + 1.7 \cdot T) \tag{4}$$

where L_{pp} is the length between perpendiculars, C_B the block coefficient, B the ship's breadth, and T the draft.

Eq. (5) expresses the air resistance (Birk, 2019):

$$R_{AA} = \frac{1}{2} \cdot C_{AA} \cdot \rho_A \cdot A_{FR} \cdot V^2 \tag{5}$$

where C_{AA} is the air resistance coefficient, ρ_A the air mass density, A_{FR} the frontal area of the ship above the waterline, and V the ship's speed. The frontal area of the ship above waterline depends on the draft:

$$A_{FR}(T) = A_F - T \cdot B \tag{6}$$

where A_{FR} is the frontal area of the ship above the waterline, A_F the front area of the lengthwise projection of hull and superstructure, T is the average draft, and B is the breadth of the ship.

Regarding the added resistance due to weather conditions, Eq. (7) expresses the added wind resistance, depending on the wind speed v_W,

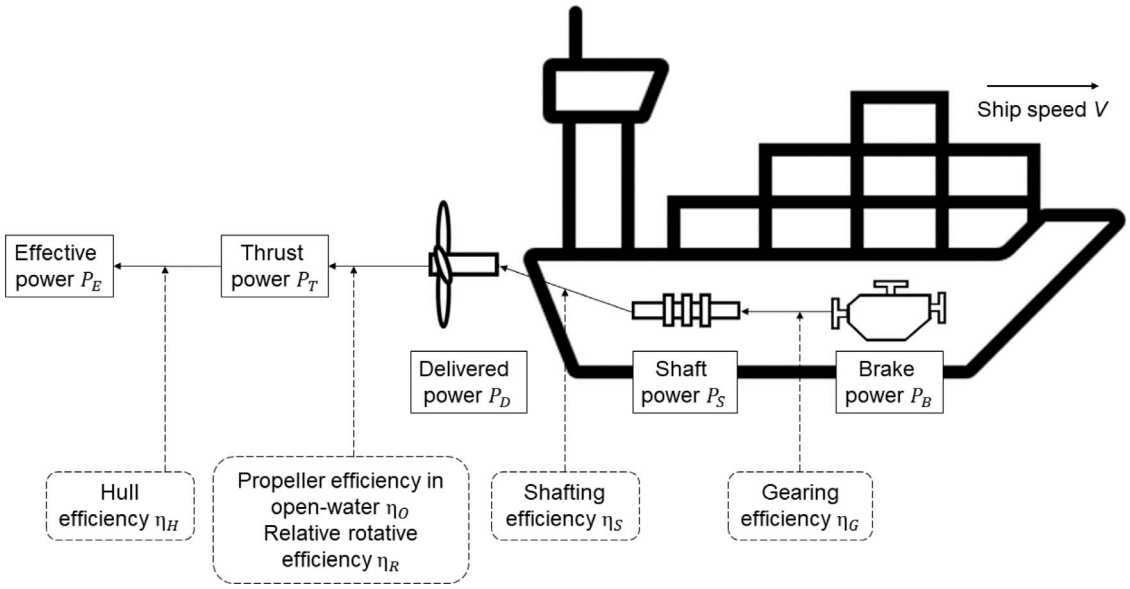

Fig. 11. A ship's propulsion system. Own representation based on Birk (2019).

and the air resistance coefficient C_{AA} changes according to the wind direction α (Birk, 2019):

$$\Delta R_{wind} = \frac{1}{2} \cdot C_{AA}(\alpha) \cdot \rho_A \cdot A_{FR}(T) \cdot v_W^2 \tag{7}$$

Following IMO (2021b), Eq. (8) expresses the added resistance in irregular short-crested waves (not applicable to swells), and for wave directions from 0 to 30° relative to the bow:

$$R_{WaveBow} = 1336 \cdot (5.3 + V) \cdot \left(\frac{B \cdot T}{L_{pp}}\right)^{0.75} \cdot h_S^2 \tag{8}$$

where B is the breadth of ship, L_{pp} the length between perpendiculars, T the draft at the specified condition of loading, h_S the significant wave height, and V the ship speed.

Therefore, the resistances are modeled as normal distributions, where the means are obtained from Eqs. (3) to (8).

$$R_F \sim \mathcal{N}(\frac{1}{2} \cdot C_F \cdot \rho \cdot S \cdot X_{Speed}^2, 1)$$
$$A_{FR}(T) = A_F - T \cdot B$$
$$R_{AA} \sim \mathcal{N}(\frac{1}{2} \cdot C_{AA} \cdot \rho_A \cdot A_{FR}(T) \cdot X_{Speed}^2, 1)$$
$$\Delta R_{wind} \sim \mathcal{N}(\frac{1}{2} \cdot C_{AA}(\alpha) \cdot \rho_A \cdot A_{FR}(T) \cdot X_{Wind}^2, 1)$$
$$R_{WaveBow} \sim \mathcal{N}(1336 \cdot (5.3 + X_{Speed}) \cdot \left(\frac{B \cdot d}{L_{pp}}\right)^{0.75} \cdot X_{WaveBow}^2, 1)$$

Calculating wave resistance from directions other than head wave and the swell resistance requires complex formulas that demand high computational power. Therefore, the fuel consumption of these variables is approximated analogously to the linear and polynomial models.

$$\beta_{WaveBeam}, \beta_{SwellBeam} \sim \mathcal{N}(0, 1)$$
$$\beta_{WaveStern}, \beta_{SwellStern} \sim \mathcal{N}(0, 1, b = 0)$$
$$\beta_{SwellBow} \sim \mathcal{N}(0, 1, a = 0)$$

Eq. (2) determines the brake-specific fuel consumption. The company provides the formula for the specific fuel oil consumption as a function of power requirements, indicated as $f_{foc}()$. The formula is based on the polynomial relation between power and fuel consumption, in the form $f_{foc}(P) = a + b \cdot P + c \cdot P^2 + d \cdot P^3 + e \cdot P^4$ as derived from model tests, and cannot be fully displayed here due to confidentiality agreements. Note that the wind resistance R_{Wind} is calculated based on the apparent wind speed and therefore includes the added wind resistance and the air resistance. As such, and to isolate the fuel consumption solely caused by the wind, the fuel consumption attributed to air resistance is deducted from the overall wind-related fuel consumption. The overall efficiency η is the product of the different efficiencies introduced in Eq. (2) and retrieved from model tests (see Table 3). The gearing efficiency η_G is assumed to be 1 (Birk, 2019).

$$\eta = \eta_H \cdot \eta_R \cdot \eta_O \cdot \eta_S \cdot \eta_G$$
$$foc_F = f_{foc}(\frac{R_F \cdot X_{Speed}}{\eta})$$
$$foc_{AA} = f_{foc}(\frac{R_{AA} \cdot X_{Speed}}{\eta})$$
$$foc_{Wind} = f_{foc}(\frac{\Delta R_{wind} \cdot X_{Speed}}{\eta}) - foc_{AA}$$
$$foc_{Wave} = f_{foc}(\frac{R_{WavesBow} \cdot X_{Speed}}{\eta}) + \beta_{WaveBeam} \cdot X_{WaveBeam}^2 + \beta_{WaveStern} \cdot X_{WaveStern}^2$$
$$foc_{Swell} = \beta_{SwellBow} \cdot X_{SwellBow}^2 + \beta_{SwellBeam} \cdot X_{SwellBeam}^2 + \beta_{SwellStern} \cdot X_{SwellStern}^2$$

The remaining specifications of the probabilistic model are given below:

$$\beta_0 \sim \mathcal{N}(0, 1)$$
$$\mu = \beta_0 + foc_F + foc_{AA} + foc_{Wind} + foc_{Wave} + foc_{Swell}$$
$$\sigma \sim \mathcal{N}(0, 1, a = 0)$$
$$y \sim \mathcal{N}(\mu, \sigma, a = 0)$$

The different models (linear with/without directions, polynomial with/without directions, and grey-box) are implemented in Python 3.8.5, using the probabilistic programming software package PyMC by Salvatier et al. (2016).

The original noon reports data set is divided into a training and a test data set, with the training set containing 80% of the original data. Using PyMC, explanatory variables can be replaced with the test data after training, which enables the user to make predictions for the test data using the model trained on the training data (The PyMC Development Team, 2023). From these predictions, metrics assessing the model performance, introduced in Section 3.4, are calculated using the scikit-learn library (Pedregosa et al., 2011). The ArviZ library complements the previous library by providing a Pareto-smoothed importance sampling leave-one-out cross-validation method, introduced in Section 3.4 (Kumar et al., 2019).

Table 4
Performance comparison between the models.

Model	R^2	MAE	MAPE	elpd
Linear - No direction	0.835	0.358 t/h	12.5%	−638
Linear - Direction	**0.875**	0.289 t/h	10.5%	−534
Polynomial - No direction	0.839	0.347 t/h	11.4%	−614
Polynomial - Direction	0.866	0.305 t/h	10.1%	−509
Grey-box model	0.874	**0.283 t/h**	**10.0%**	−485

3.4. Model evaluation

This section evaluates the predictive performance of the different models to determine the most appropriate one. Three evaluation metrics are chosen: the coefficient of determination (R^2 score), the Mean Absolute Error (MAE), and the Mean Absolute Percentage Error (MAPE). The R^2 score describes the share of the total variance explained by the model and measures a model's overall fit to the data. The MAE represents the mean of the errors, i.e., the differences between the observed and predicted values for all data points. The MAPE calculates the error divided by the actual target variable, averaged over all data points, which puts the expected deviation from the actual fuel consumption into the perspective of the overall fuel consumption. Additionally, the Pareto-smoothed importance sampling leave-one-out cross-validation method, provided by the Arviz library (Kumar et al., 2019), estimates the expected log pointwise predictive density (elpd) for the test data. The higher the elpd value, the better the models' accuracy in predicting the test data. Table 4 shows the obtained performance metrics for all models.

Fig. 12 shows a graphical representation of the models' data fit, only for the models with directions, which are more accurate than those without directions for all four metrics, and the grey-box model. The blue and orange lines represent the predicted fuel consumption distributions and their average. The linear model has the highest R^2, second best MAE, and third best MAPE and elpd. While this model fits well the actual distribution above two tons per hour, the fit is more inaccurate in the range from one to two tons per hour. The polynomial regression model predicts the underlying distribution well, with the second best MAPE and elpd, and third best R^2 and MAE. The grey-box model shows the best MAE, MAPE and elpd and the second highest R^2, close to the linear model, and a good fit of the actual distribution, as shown in Fig. 12.

Fig. 13 illustrates the models' fit where the models' predicted and actual fuel consumption values are plotted against each other for all three models. The figure indicates difficulty in predicting the highest fuel consumption rates, as these points are scarce in the data set. Fig. 13(a) also confirms the under-estimation of the linear model in the range between one and two tons per hour.

Based on these different results, the linear and polynomial models, which incorporate the weather directions, and the grey-box models demonstrate high and accurate predictive performance and are selected for further analysis. Given the research objective of gathering comprehensive insights into the influence of weather conditions and its higher predictive accuracy, the grey-box model is preferred in the results.

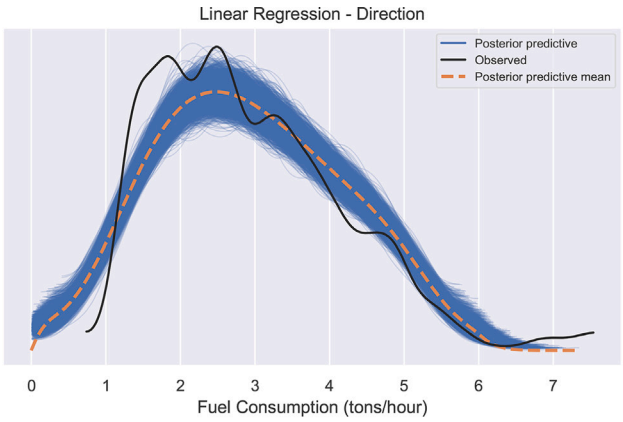

(a) Posterior predictive distribution - Linear model with weather directions

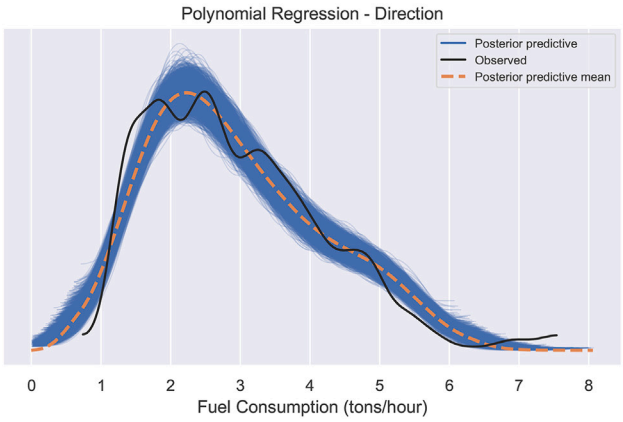

(b) Posterior predictive distribution - Polynomial model with weather directions

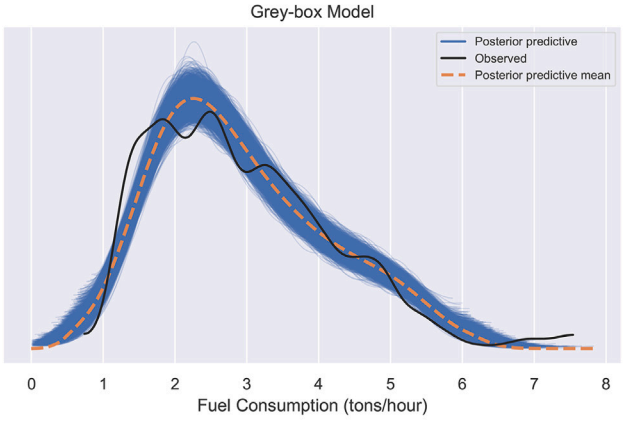

(c) Posterior predictive distribution - Grey-box model

Fig. 12. Posterior predictive distributions.

4. Results

This section presents the results concerning the impact of weather on ship fuel consumption and develops weather correction factors based on these results.

4.1. Influence of weather

Eq. (9) estimates the share of fuel consumption attributed to weather:

$$\text{Share of fuel consumption due to weather} = \frac{y_{Weather}}{y_{Total} - \hat{\beta}_0} \tag{9}$$

where $y_{Weather}$ is the fuel consumption attributed to weather, y_{Total} the total fuel consumption and $\hat{\beta}_0$ the fitted intercept term. Considering that the intercept β_0 of the fuel consumption equation should be zero (i.e., no fuel consumption if the ship is not in operation), it is assumed that the fitted value for $\hat{\beta}_0$ solely consists of the error term ϵ. Therefore, $\hat{\beta}_0$ can be subtracted from the total fuel consumption (y_{Total}) without losing information regarding the impact of weather.

Fig. 14 shows the result of the share of fuel consumption due to weather, comparing the linear, polynomial and grey-box models. The linear and polynomial models respectively report a mean of 3.7% and 7.4% of the fuel consumption attributed to weather, while this is raised

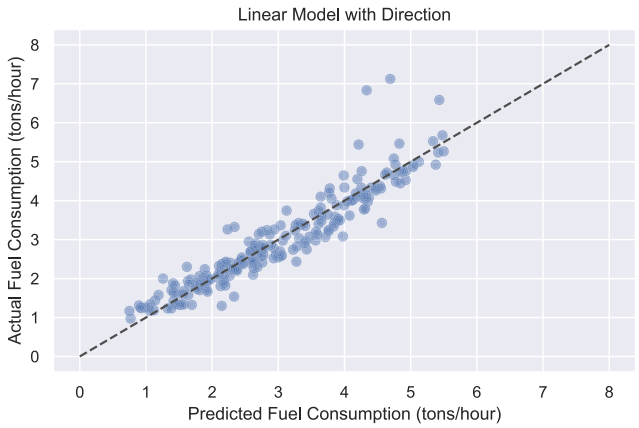

(a) Posterior predictive fit - Linear model with weather directions

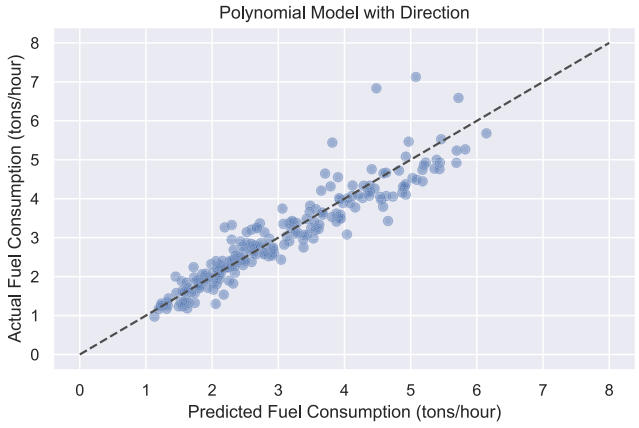

(b) Posterior predictive fit - Polynomial model with weather directions

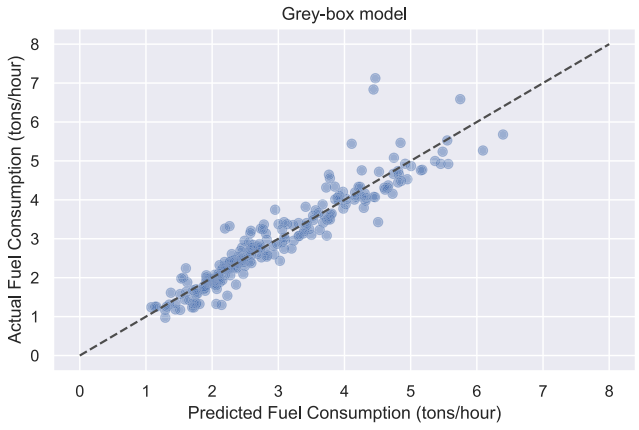

(c) Posterior predictive fit - Grey-box model

Fig. 13. Posterior predictive fits.

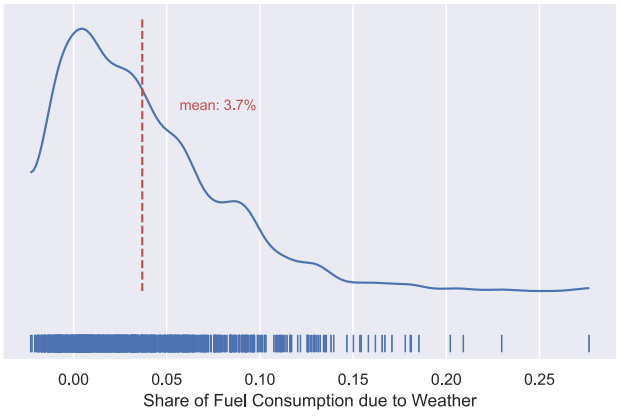

(a) Linear model with weather directions

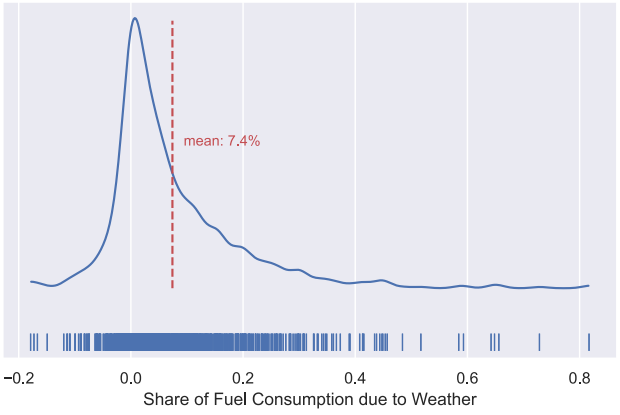

(b) Polynomial model with weather directions

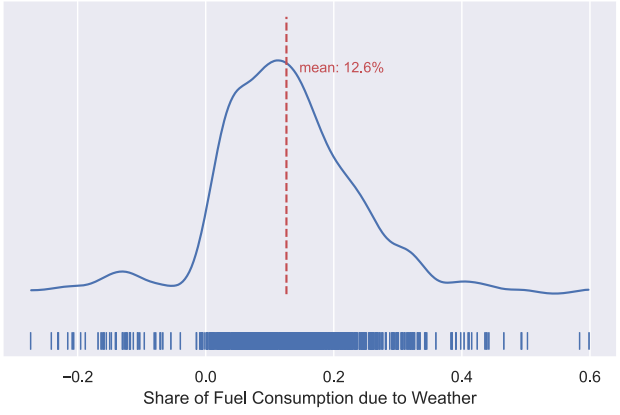

(c) Grey-box model with weather directions

Fig. 14. Distribution of the impact of weather as a share of the total fuel consumption. The vertical blue bars indicate the individual observations, and the dotted red line is the mean value.

to 12.6% for the grey-box model. Figs. 15 to 17 show the impact of each weather component (wind, wave, and swell) on the total fuel consumption, differentiated depending on the relative direction.

Fig. 15 shows that, on average, 1.2% to 2.9% of the fuel consumption can be attributed to the wind for the linear and polynomial models, with 2.6% for the grey-box model. In headwind (42.3% of the observations), the share increases to 8.4% and 9.0%, respectively for the polynomial and grey-box models, but only to 2.8% for the linear model, while it decreases to −2.3% and −5.4% (and only −0.7% for the linear model) for the stern wind (34.6% of the observations). Beam wind (23.1% of the observations) shows intermediate values, with 1.2%, 0.8% and 3.1%, respectively, for the linear, polynomial and grey-box models. The linear model significantly underestimates the wind impact on fuel consumption compared to the polynomial and grey-box models, especially for headwind and stern wind.

Fig. 16 presents the results regarding waves. According to the linear and polynomial models, the average share of fuel consumption attributed to waves is 1.6% and 1.8%. The grey-box model attributes a higher share to the impact of waves, with an overall impact of 7.2%. This share is mostly due to head waves (45.3% of the observations), with an impact of 7.7%, while this impact is more moderate for the

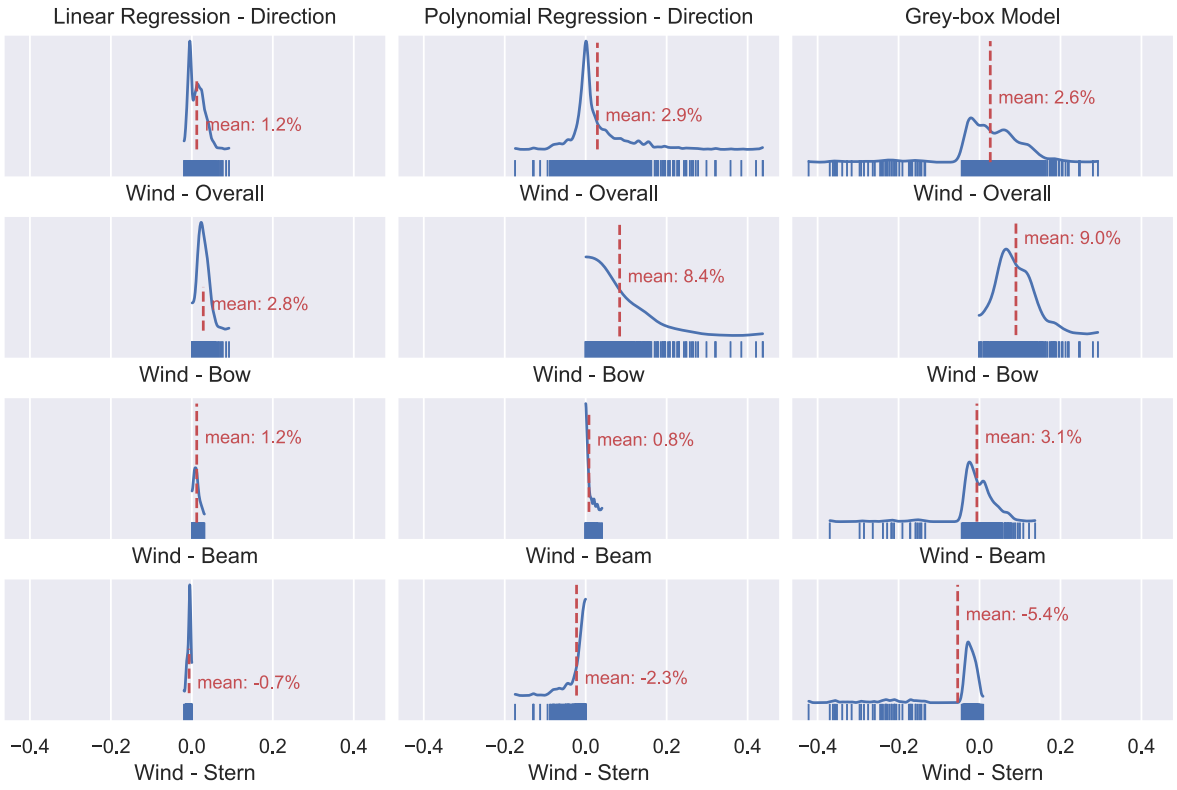

Fig. 15. Distribution of the impact of wind on fuel consumption, depending on the direction (wind directions ranging from 0° to 60° (in relation to the bow) are denoted as 'bow', 60° to 120° as 'beam', and 120° to 180° as 'stern').

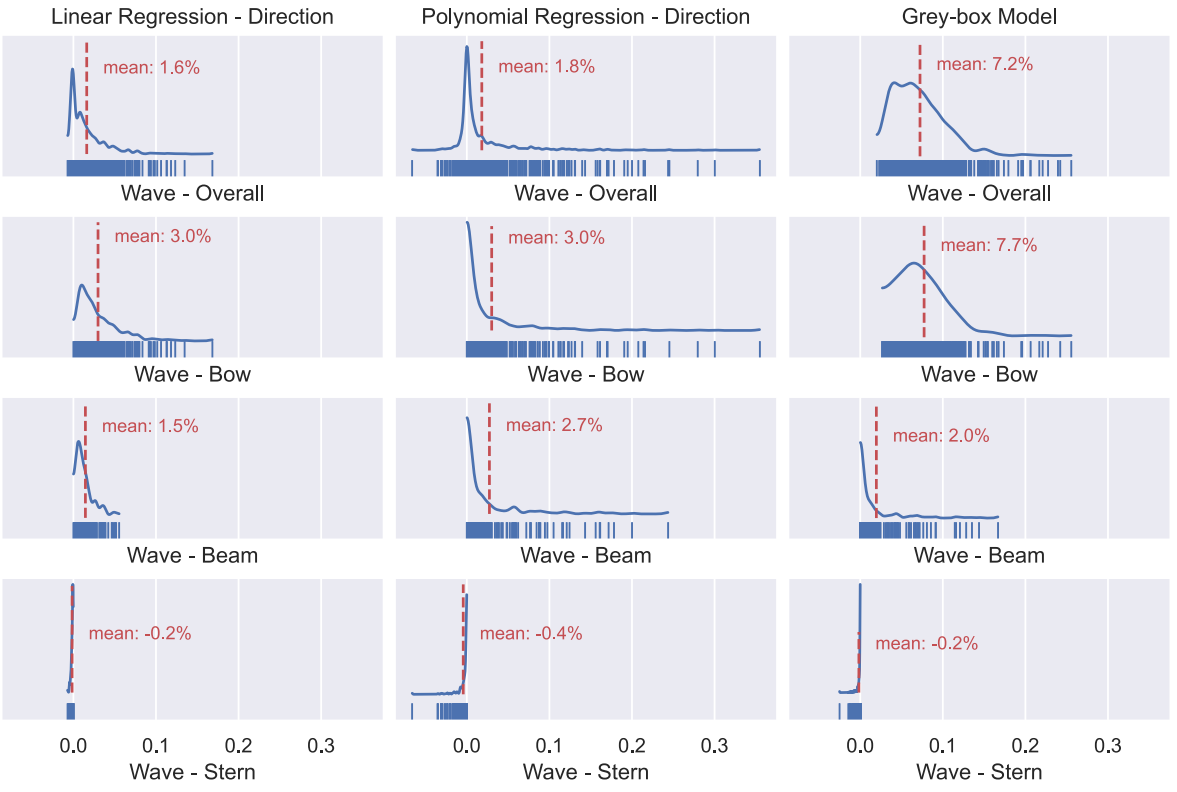

Fig. 16. Distribution of the impact of waves on fuel consumption, depending on the direction (wave directions ranging from 0° to 60° (in relation to the bow) are denoted as 'bow', 60° to 120° as 'beam', and 120° to 180° as 'stern').

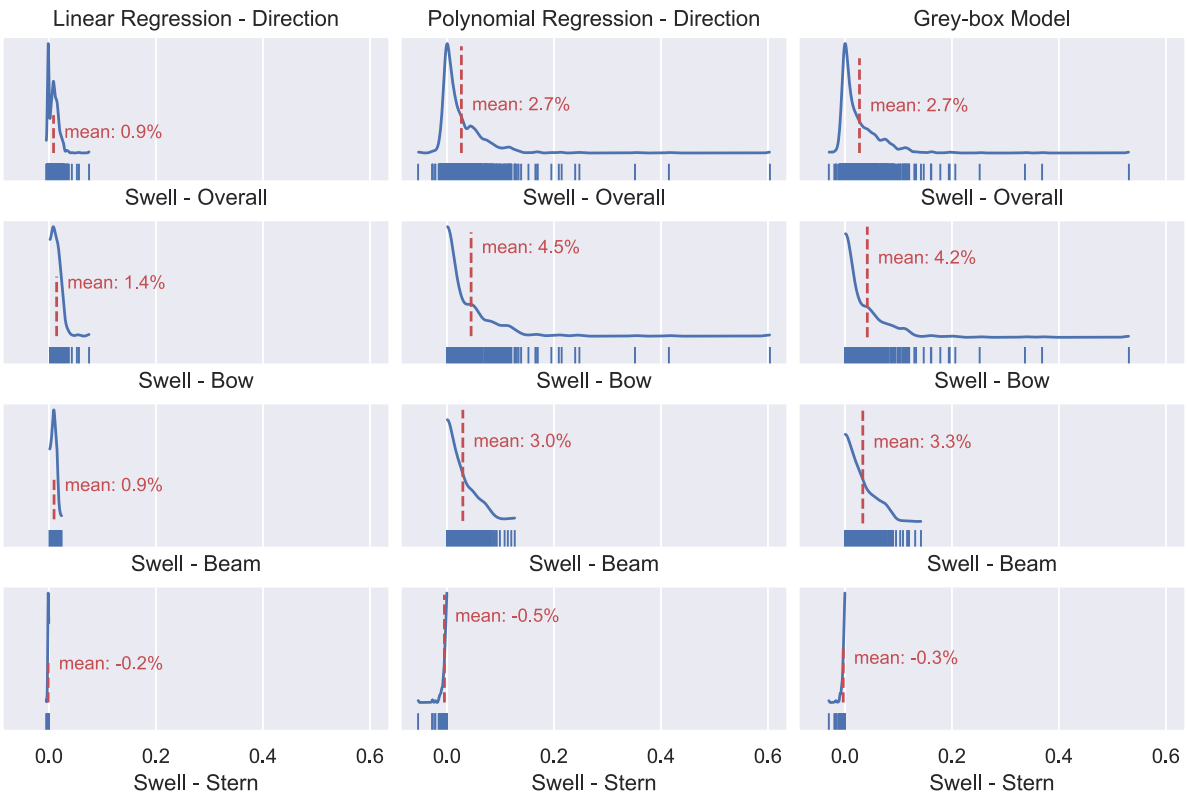

Fig. 17. Distribution of the impact of swells on fuel consumption, depending on the direction (swell directions ranging from 0° to 60° (in relation to the bow) are denoted as 'bow', 60° to 120° as 'beam', and 120° to 180° as 'stern').

linear and polynomial models (3.0% for both models). The impact of beam waves (21.7% of the observations) is lower for all models (1.5%, 2.7% and 2.0% for, respectively, the linear, polynomial and grey-box models). Finally, the share of fuel consumption attributed to stern waves (33.0% of the observations) is limited for all three models.

The overall average share of fuel consumption due to swells is 2.7% according to the polynomial and grey-box models (only 0.9% for the linear model), as shown in Fig. 17. The bow swells (41.6% of the observations) account for 4.5% and 4.2%, respectively, for the polynomial and grey-box models and only 1.4% for the linear model. Beam swells (31.8% of the observations) have a share of 3.0% and 3.3% (0.9% for the linear model), while the share for the stern swells (26.6% of the observations) falls to −0.5% and −0.3% for the polynomial and grey-box models, and also −0.2% for the linear model. Like with the wind impact, the linear model underestimates the impact of swells compared to the polynomial and grey-box models, which give similar estimations.

Figs. 18–20 present the influence of weather on fuel consumption for the different sea states, respectively, for the linear, polynomial, and grey-box models. The numbers in parentheses indicate the wind speeds related to the respective sea state. As seen previously, the linear model estimates less impact from the weather compared to the other two models, ranging from 1.4% for BF 0 to 8.2% for BF 7. The polynomial model indicates the broadest range of estimation from 2.4% for BF 0 to 20.4% for BF 7. Finally, the grey-box model shows the highest estimate for low BF numbers (9.1% for BF 0) and goes up to 16.2% for BF 7. The polynomial and grey-box models estimate figures for BF 5 and 6 that are close to the margin of 15% taken as a reference by the IMO (Faber et al., 2020), which is not the case for the linear model. This is an additional reason for excluding the linear model from further analysis.

4.2. Weather correction factors

This section develops different weather correction factors for various sea states to address the shortcomings of having a single sea state presented in . These correction factors follow the same formulation with the EEDI weather correction factor f_w, meaning that the factors are meant for the EEDI denominator and with a value between zero and one (one corresponding to calm-sea conditions). Note that the weather correction factors decrease as the weather conditions get harsher. For comparison purposes, the IMO weather correction factor f_w is also calculated through the reference line for container ships (IMO, 2012b):

$$f_w = 0.0208 \cdot \ln(\text{Capacity}) + 0.633 \tag{10}$$

The correction factor for each sea state is obtained by dividing the fuel consumption of calm water by the fuel consumption of the corresponding sea condition. Eq. (11) expresses the correction factor as a function of Share of $y_{Weather}$. It defines weather-related fuel consumption as a share of the total fuel consumption and results directly from the analysis of the previous section.

$$\text{Weather correction factor} = 1 - \text{Share of } y_{Weather} \tag{11}$$

The correction factors are calculated based only on the results of the polynomial and grey-box models, using results from Figs. 19 and 20. Table 5 provides the sea state-specific correction factors and compares them with the mean of the sample voyages (from the noon reports) and the IMO weather correction factor f_w.

According to Table 5, the influence of weather conditions from the polynomial model is minimal for BF 0 to BF 1. However, it notably increases with each subsequent step from BF 3 to BF 7. This aligns with the model following a quadratic function for the weather variables. The weather correction factors decrease correspondingly. For the grey-box model, the impact is not as spread between low and high BF numbers. Using the grey-box model, the weather correction factor for the sample voyages (0.874) gets very close to the IMO f_w of 0.875 for the sample ships.

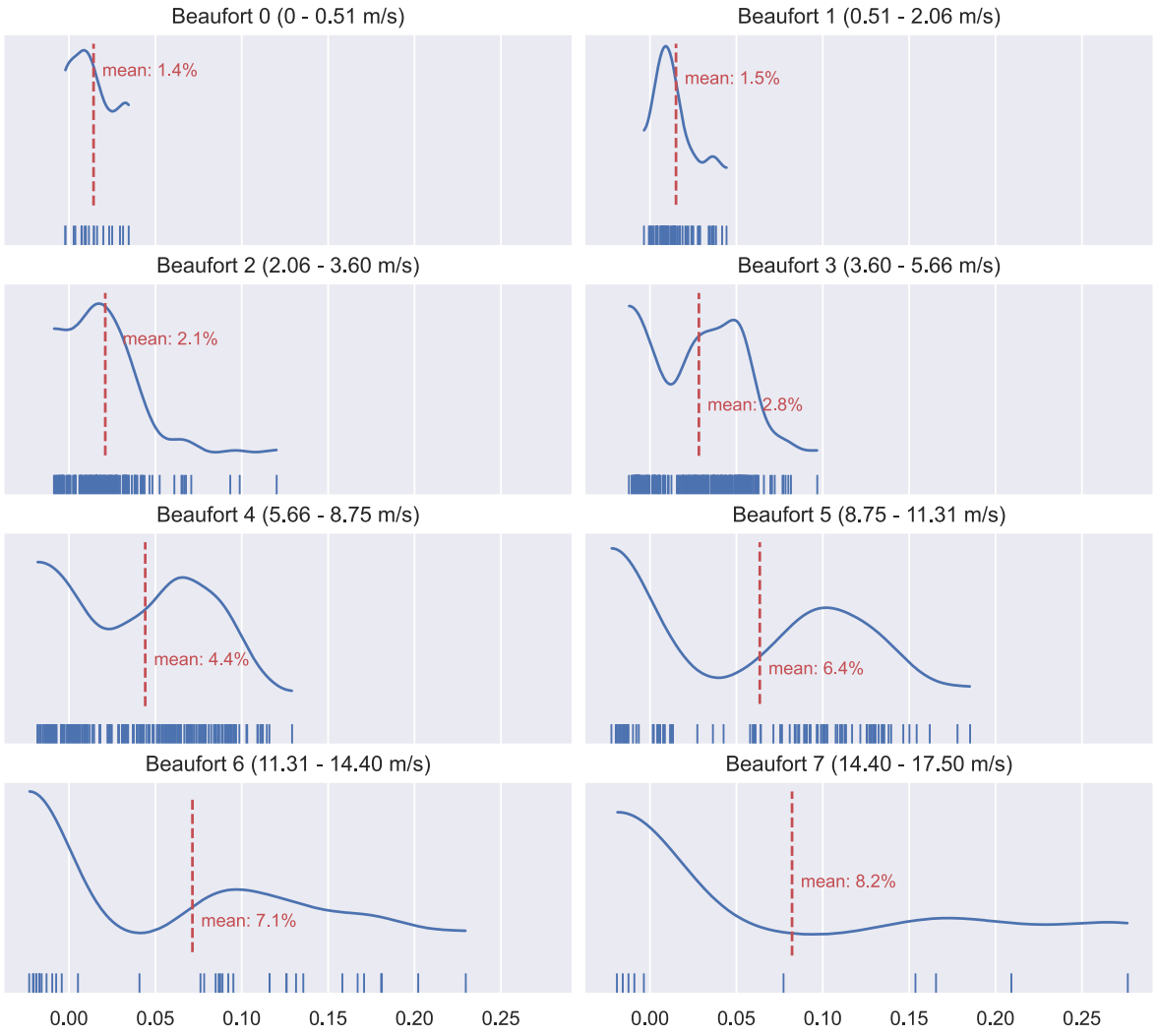

Fig. 18. Weather impact on fuel consumption by sea state — Linear model.

Table 5
Correction factor for different sea states.

Sea state	Correction factor		Weather impact	
	Polynomial	Grey-box	Polynomial	Grey-box
Beaufort 0	0.976	0.909	2.4%	9.1%
Beaufort 1	0.976	0.900	2.4%	9.9%
Beaufort 2	0.962	0.893	3.8%	10.7%
Beaufort 3	0.950	0.883	4.9%	11.7%
Beaufort 4	0.911	0.861	8.9%	13.9%
Beaufort 5	0.857	0.847	14.3%	15.3%
Beaufort 6	0.834	0.842	16.6%	15.8%
Beaufort 7	0.796	0.839	20.4%	16.2%
Sample voyages	0.926	0.874	7.4%	12.6%
f_w from IMO	0.875		12.5%	

5. Discussion

This section discusses the policy implications of weather correction factors, compares the findings with existing literature, and presents the limitations of the study.

5.1. Policy implications of weather correction factors

The weather correction factors derived from operational data are compared with the IMO factor f_w. The results of the polynomial model from Table 5 indicate a significant growth in the weather impact for BF numbers greater than three. While the incremental step between sea states is more constant for the grey-box model (except for a higher variation from Beaufort 3 to 4), choosing the representative sea state for a correction factor is crucial. For instance, BF 6, adopted by IMO as a reference, is not the most encountered sea state of this study's sample and does not match the average wind speed from Fig. 1, corresponding to BF 4 (5.5 to 7.9 m s^{-1}). This is also not the case in Bialystocki and Konovessis (2016), where the most common condition is BF 5. Nevertheless, the correction factors are only derived using data from two sister container ships and vary depending on different model estimations, necessitating further analysis for broader applicability across various ship types and sizes.

Different approaches can develop the current work further. From a technical point of view and considering weather correction factors for EEDI, a set of correction factors for different sea states could improve the reliability of this energy efficiency indicator. Different EEDI requirements could become mandatory for various weather conditions, as suggested by Bøckmann and Steen (2016). Lindstad et al. (2019) also advocate for a revision of the EEDI definition to include requirements for weather conditions.

To achieve fairer benchmarking, an operational indicator such as CII could be corrected using the weather correction factor corresponding to the most encountered sea state. Alternatively, the weather correction factor could be estimated as a weighted average across the sea states faced rather than selecting the most frequent one. Weather correction

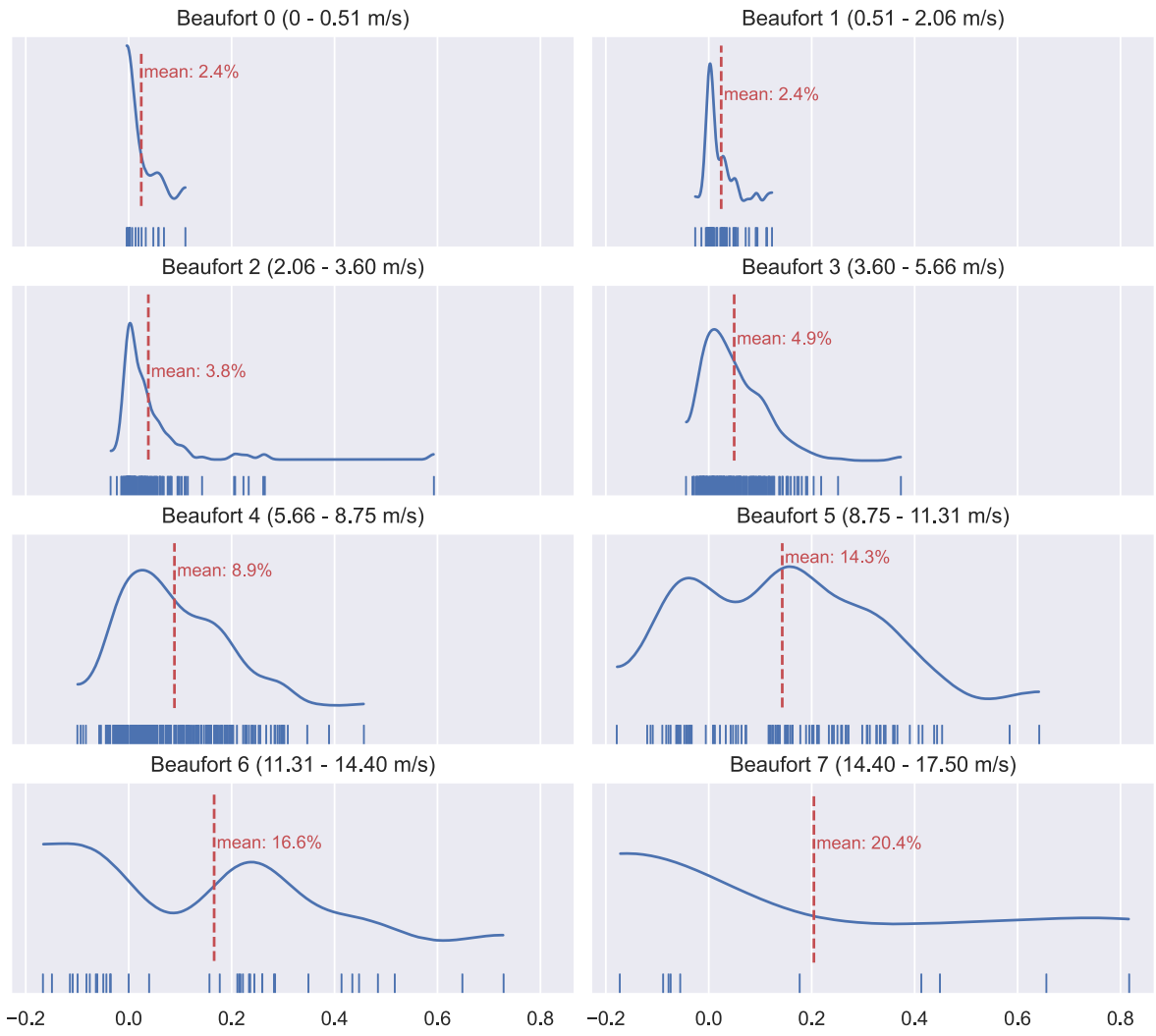

Fig. 19. Weather impact on fuel consumption by sea state — Polynomial model.

factors can also be combined with other approaches to operational indicators, such as operational cycles (Godet et al., 2023) or real-time monitoring of energy efficiency (Chi et al., 2018).

In any event, corrections to the energy efficiency indicators, such as those suggested above, can only be adopted by international policy-making institutions after exhaustive technical and political discussions. These discussions can only be based on analyses performed by properly certified organizations (i.e., classification societies) that have access to verified data from a ship sample much larger and diverse than the one used for the present study. In this sense, the contribution of the present study mainly concerns the methodology applied and the initiation of the relevant scientific dialogue.

5.2. Comparison with existing literature

Meng et al. (2016) estimate the effect of bad weather (defined as bow/beam waves of 2.5 m or higher) on the fuel consumption of four container ships. When considering all directions, they find that bad weather (BF 5 or higher) contributes between 4 and 10% to the fuel consumption of the ships examined. These numbers rise to 6%–20% when counting only for wind and waves from bow and beam (Meng et al., 2016). Their estimations are more in line with the results of the linear model of the present analysis, which range from 6.4% (for BF 5) to 8.2% (for BF 7). The estimates deriving from the polynomial and grey-box models are about twice as high.

Studies using Computational Fluid Dynamics (CFD) tend to estimate higher numbers for the weather effect on fuel consumption than this study. For example, Islam and Guedes Soares (2022) study a KRISO container ship and find that the required propulsion power for BF 3 is 42% above the estimated one for calm sea. The CFD analysis of an S175 container ship by Kim et al. (2017) results in a sea margin between 17% at 23 knots and 34% at 16 knots, for BF 6 with headwind and waves. It is worth mentioning that the relatively fewer observations with BF 6 or higher in the data set analyzed here (refer to Fig. 8) challenges the reliability of the resulting estimates for these sea states. In any case, however, none of the models examined here come even close to these numbers.

5.3. Limitations

There are several limitations of this study worth mentioning. First, noon reports are often challenged for their uncertainties due to the low data frequency and the manual reporting of many variables (Aldous et al., 2013). The uncertainties of hindcast weather data must also be considered (Vettor and Guedes Soares, 2022). While noon reports allow for estimations over a large period (two years), the availability of high-frequency data could complement and refine the analysis conducted in this study.

Second, other operational factors that influence fuel consumption are excluded from the analysis. For example, the influence of trim

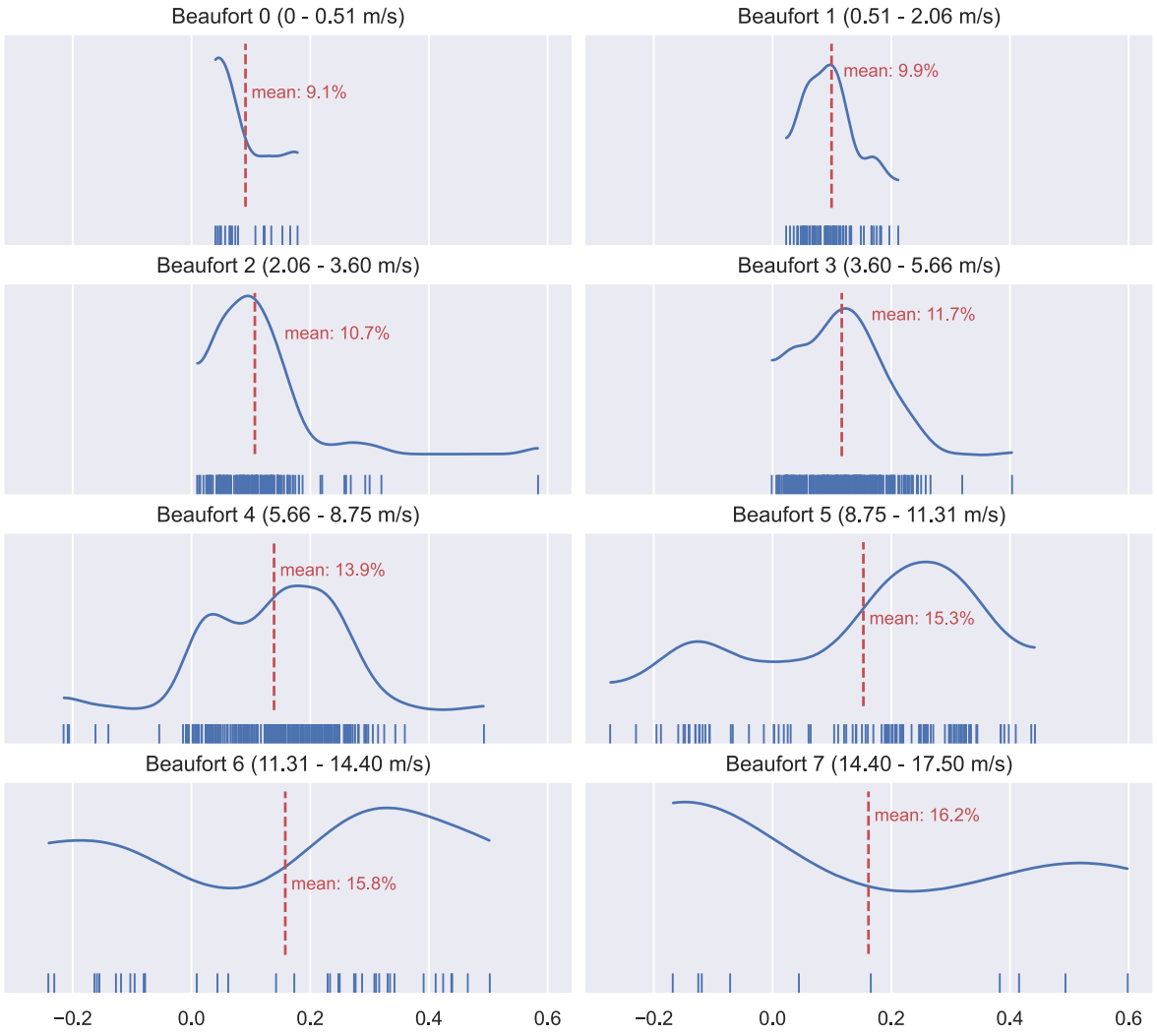

Fig. 20. Weather impact on fuel consumption by sea state — Grey-box model.

varies with the draft and the ship's speed. Using CFD, Islam and Guedes Soares (2019) find a difference between 0 and 4% in calm-water resistance when changing the draft and trim angle. For hull fouling, Adland et al. (2018) indicate a 9% savings in fuel consumption by hull cleaning. However, as the present data set only covers two years, analyzing the effect of dry-docking or other maintenance operations is impossible. The impact of biofouling and other latent factors is likely captured in the error term in this analysis. Moreover, water depth is an essential parameter for inland and shallow water transport. The present study restricts itself to observations concerning ships sailing in the open deep sea.

Third, regarding the models, linear regressions assume the independence of variables. However, as shown in Fig. 9, wave height/direction are, to some extent, correlated with wind speed/direction. Ship speed exhibits a similar issue. It cannot be considered independent from weather, as a ship would sail slower in harsh weather conditions and/or due to lower visibility (Psaraftis and Lagouvardou, 2023). It is worth noting, however, that unexpectedly Fig. 9 shows a positive, albeit very weak, correlation of ship speed (through water) with the weather components; the relative wind direction is the only exception. This is probably due to the fact that sailing segments close to the coast, where ships usually slow down in adverse conditions, have been excluded from the analysis. Sailing in coastal and other shallow waters is an area that future research should explore in relation to investigating the weather impact on fuel consumption and energy efficiency.

Fourth, the fuel consumption estimates and the corresponding energy efficiency values mentioned in the present study are based solely on the operation of the main engine(s) of the ship. The effect of weather on the fuel consumption of auxiliary engines is another subject that future research should investigate.

Furthermore, as already mentioned in Section 5.1, the study aims at initiating an approach to a broader discussion on the influence of weather on energy efficiency indicators. Substantial analysis of additional data on different ship types and sizes, as well as different geographical regions, will be necessary before any formal policy application.

6. Conclusions

International shipping contributes significantly to GHG emissions, burning fossil fuels to transport goods. The IMO regulations intend to reduce these emissions by setting energy efficiency standards, using technical (EEDI) and operational (CII) indicators. Energy efficiency and fuel consumption depend on many operational factors, including weather conditions, which are mostly uncontrollable by the operators (weather routing is an effective practice but remains a reactive approach). Isolating the influence of weather is essential for ensuring harmonized benchmarking through these indicators. This study estimates the influence of weather on fuel consumption and develops factors for energy efficiency indicators to account for this influence.

Based on the analysis of noon reports of two sister container ships, key conclusions can be summarized as follows:

- Linear and polynomial regression models and a grey-box model using prior knowledge of ship hydrodynamics were developed using model-based machine learning. While the polynomial and grey-box models showed similar results, the latter presents the best accuracy on most metrics.
- The models showed a 7.4 to 12.6% average influence of weather on fuel consumption. These numbers result from two-year data, with most data points coming from moderate sea conditions (sea states 3 and 4 on the Beaufort scale). The influence of weather on main engine fuel consumption spans from 2.4% of the consumption for Beaufort 0 to 20.4% for Beaufort 7 for the polynomial model and from 9.1% to 16.2% for the grey-box model. No observations were reported above Beaufort 7, noting that the reported weather conditions are averaged over the report duration (about 24 h).
- Weather correction factors were calculated for the different sea conditions and compared with the IMO weather correction factor f_w. The average correction factor during the sample voyages is 0.926 for the polynomial model and 0.874 for the grey-box model, very close to the 0.875 figure of IMO's f_w. The resulting factors span from 0.976 for Beaufort 1 to 0.796 for Beaufort 7 for the polynomial model and 0.909 to 0.839 for the grey-box model.

This study brings a different perspective on energy efficiency indicators by considering weather correction factors differentiated for specific sea states. The need to consider the influence of weather on these indicators is emphasized if the latter are to be used for benchmarking, as is the case with EEDI/EEXI and CII. More specifically, the EEDI definition should be expanded to include energy efficiency standards for sea states different than Beaufort 0 and Beaufort 6 that is the case today. This will become possible if weather correction factors for all sea states are calculated along the lines suggested here. This is expected to result in better ship designs that take into consideration their performance under all possible weather conditions. In relation to CII, a compound weather correction factor estimated as a weighted average across the actual sea states encountered by a ship during a calendar year can nullify the effect of weather and render the indicator better suited for benchmarking as reflecting the performance of a ship on aspects only within the control of the operator.

The present analysis, however, is insufficient to support formal policy applications of such extent. This is because it aspires to be only an initial study presenting the concept and suggesting a methodology based on a very thin sample. Substantial further research is required to include: (i) much more frequent ship data than noon reports, probably supported by Automatic Identification System (AIS) and meteorological databases, (ii) investigation of the weather effects while sailing in coastal and shallow waters, (iii) investigation of other weather-related factors such as water salinity and temperature, (iv) investigation of weather effects on the fuel consumption of auxiliary engines, (v) handling estimation errors imposed by the correlation among explanatory variables including the effect of weather on ship speed (to account for reduced visibility, etc.), (vi) expansion to different ship types and sizes, and (vii) expansion to different geographical regions. On top of that, the analysis should be performed by certified institutions with access to verified data.

CRediT authorship contribution statement

Amandine Godet: Writing – original draft, Visualization, Investigation, Formal analysis, Data curation, Conceptualization. **Lukas Jonathan Michael Wallner:** Visualization, Methodology, Investigation, Formal analysis, Conceptualization. **George Panagakos:** Writing – review & editing, Validation, Supervision, Methodology, Funding acquisition, Conceptualization. **Michael Bruhn Barfod:** Writing – review & editing, Supervision, Project administration, Methodology, Funding acquisition, Conceptualization.

Declaration of competing interest

The authors declare that they have no known competing financial interests or personal relationships that could have appeared to influence the work reported in this paper.

Data availability

The data that has been used is confidential.

Acknowledgments

The authors thank the project company for sharing data and valuable knowledge and the Danish Maritime Fund's financial support under the NICE project, grant number 2020-024.

References

Adland, R., Cariou, P., Jia, H., Wolff, F.-C., 2018. The energy efficiency effects of periodic ship hull cleaning. J. Clean. Prod. 178, 1–13. http://dx.doi.org/10.1016/j.jclepro.2017.12.247, https://linkinghub.elsevier.com/retrieve/pii/S0959652617332419.

Aldous, L., Smith, T., Bucknall, R., 2013. Noon report data uncertainty. In: Low Carbon Shipping Conference. London, UK.

Berthelsen, F.H., Nielsen, U.D., 2021. Prediction of ships' speed-power relationship at speed intervals below the design speed. Transp. Res. D 99, 102996. http://dx.doi.org/10.1016/J.TRD.2021.102996, https://www.sciencedirect.com/science/article/pii/S1361920921002947?via%3Dihub.

Bialystocki, N., Konovessis, D., 2016. On the estimation of ship's fuel consumption and speed curve: A statistical approach. J. Ocean Eng. Sci. 1, 157–166. http://dx.doi.org/10.1016/j.joes.2016.02.001, https://www.sciencedirect.com/science/article/pii/S2468013315300127.

Bilgili, L., 2023. Determination of the weights of external conditions for ship resistance. Ocean Eng. 276, 114141. http://dx.doi.org/10.1016/j.oceaneng.2023.114141, https://linkinghub.elsevier.com/retrieve/pii/S0029801823005255.

Birk, L., 2019. Fundamentals of Ship Hydrodynamics. Wiley, http://dx.doi.org/10.1002/9781119191575, https://onlinelibrary.wiley.com/doi/book/10.1002/9781119191575.

Bishop, C.M., 2013. Model-based machine learning. Phil. Trans. R. Soc. A 371, 20120222. http://dx.doi.org/10.1098/rsta.2012.0222, https://royalsocietypublishing.org/doi/10.1098/rsta.2012.0222.

Bocchetti, D., Lepore, A., Palumbo, B., Vitiello, L., 2015. A statistical approach to ship fuel consumption monitoring. J. Ship Res. 59 (3), 162–171. http://dx.doi.org/10.5957/JOSR.59.3.150012, http://www.ingentaselect.com/rpsv/cgi-bin/cgi?ini=xref&body=linker&reqdoi=10.5957/JOSR.59.3.150012.

Bøckmann, E., Steen, S., 2016. Calculation of EEDIweather for a general cargo vessel. Ocean Eng. 122, 68–73. http://dx.doi.org/10.1016/j.oceaneng.2016.06.007.

Chi, H., Pedrielli, G., Ng, S.H., Kister, T., Bressan, S., 2018. A framework for real-time monitoring of energy efficiency of marine vessels. Energy 145, 246–260. http://dx.doi.org/10.1016/j.energy.2017.12.088, https://linkinghub.elsevier.com/retrieve/pii/S036054421732131X.

Du, Y., Meng, Q., Wang, S., Kuang, H., 2019. Two-phase optimal solutions for ship speed and trim optimization over a voyage using voyage report data. Transp. Res. B 122, 88–114. http://dx.doi.org/10.1016/j.trb.2019.02.004.

Faber, J., Hanayam, S., Zhang, S., Pereda, P., Comer, B., Hauerhof, E., Schim van der Loeff, W., Smith, T., Zhang, Y., Kosaka, H., Adachi, M., Bonello, J.-M., Galbraith, C., Gong, Z., Hirata, K., Hummels, D., Kleijn, A., Lee, D.S., Liu, Y., Lucchesi, A., Mao, X., Muraoka, E., Osipova, L., Qian, H., Rutherford, D., Suárez de la Fuente, S., Yuan, H., Velandia Perico, C., Wu, L., Sun, D., Yoo, D.-H., Xing, H., 2020. Fourth IMO Greenhouse Gas Study 2020. Tech. Rep., International Maritime Organization, London, UK, p. 295.

Fan, A., Wang, Y., Yang, L., Tu, X., Yang, J., Shu, Y., 2024. Comprehensive evaluation of machine learning models for predicting ship energy consumption based on onboard sensor data. Ocean Coast. Manag. 248, 106946. http://dx.doi.org/10.1016/j.ocecoaman.2023.106946, https://linkinghub.elsevier.com/retrieve/pii/S0964569123004714.

Fan, A., Yang, J., Yang, L., Wu, D., Vladimir, N., 2022. A review of ship fuel consumption models. Ocean Eng. 264, 112405. http://dx.doi.org/10.1016/j.oceaneng.2022.112405, https://linkinghub.elsevier.com/retrieve/pii/S0029801822016936.

Godet, A., Nurup, J.N., Saber, J.T., Panagakos, G., Barfod, M.B., 2023. Operational cycles for maritime transportation: A benchmarking tool for ship energy efficiency. Transp. Res. D 121, 103840. http://dx.doi.org/10.1016/j.trd.2023.103840, https://linkinghub.elsevier.com/retrieve/pii/S1361920923002377.

Grlj, C.G., Degiuli, N., Tuković, Ž., Farkas, A., Martić, I., 2023. The effect of loading conditions and ship speed on the wind and air resistance of a containership. Ocean Eng. 273, 113991. http://dx.doi.org/10.1016/J.OCEANENG.2023.113991.

Hu, Z., Jin, Y., Hu, Q., Sen, S., Zhou, T., Osman, M.T., 2019. Prediction of fuel consumption for enroute ship based on machine learning. IEEE Access 7, 119497–119505. http://dx.doi.org/10.1109/access.2019.2933630.

Hu, Z., Zhou, T., Osman, M.T., Li, X., Jin, Y., Zhen, R., 2021. A novel hybrid fuel consumption prediction model for ocean-going container ships based on sensor data. J. Mar. Sci. Eng. 9 (4), 449. http://dx.doi.org/10.3390/jmse9040449, https://www.mdpi.com/2077-1312/9/4/449.

IMO, 2009. Comments on the coefficient "fw" in the EEDI formula. In: Resolution MEPC 59/4/21. International Maritime Organization, London, UK, (May).

IMO, 2012a. Draft guidelines for the calculation of the coefficient fw for decrease in ship speed in a representative sea condition. In: MEPC 64/4/38. p. 2.

IMO, 2012b. Interim guidelines for the calculation of the coefficient fw for decrease in ship speed in a representative sea condition for trial use. In: Resolution MEPC.1/Circ.796. International Maritime Organization, London, UK.

IMO, 2019. 2019 Guidelines for consistent implementation of the 0.50% sulphur limit under MARPOL annex VI. In: Resolution MEPC.320(74). International Maritime Organization, London, UK, https://wwwcdn.imo.org/localresources/en/KnowledgeCentre/IndexofIMOResolutions/MEPCDocuments/MEPC.320%2874%29.pdf.

IMO, 2021a. CII reduction factors. In: MEPC 76/7/33. p. 7.

IMO, 2021b. Guidelines for determining minimum propulsion to maintain the manoeuvrability of ships in adverse conditions. In: Resolution MEPC.1/Circ.850/Rev.3. International Maritime Organization, London, UK, https://wwwcdn.imo.org/localresources/en/OurWork/Environment/Documents/Air%20pollution/MEPC.1-Circ.850-Rev.3.pdf.

IMO, 2023. 2023 IMO strategy on reduction of GHG emissions from ships. In: Resolution MEPC.377(80). International Maritime Organization, London, UK, https://wwwcdn.imo.org/localresources/en/MediaCentre/PressBriefings/Documents/Clean%20version%20of%20Annex%201.pdf.

Islam, H., Guedes Soares, C., 2019. Effect of trim on container ship resistance at different ship speeds and drafts. Ocean Eng. 183, 106–115. http://dx.doi.org/10.1016/j.oceaneng.2019.03.058, https://linkinghub.elsevier.com/retrieve/pii/S0029801819301477.

Islam, H., Guedes Soares, C., 2022. Head wave simulation of a KRISO container ship model using OpenFOAM for the assessment of sea margin. J. Offshore Mech. Arct. Eng. 144 (3), http://dx.doi.org/10.1115/1.4053538, https://asmedigitalcollection.asme.org/offshoremechanics/article/144/3/031902/1131327/Head-Wave-Simulation-of-a-KRISO-Container-Ship.

ISO, 2015. BS ISO 15016:2015 - annex B: Beaufort scale for wind velocity.

ITTC, 2021. ITTC Symbols and Terminology List. Tech. Rep., International Towing Tank Conference, https://ittc.info/media/9880/structured-list_2021_a.pdf.

James, G., Witten, D., Hastie, T., Tibshirani, R., 2023. An Introduction to Statistical Learning with Applications in R Second Edition. Springer New York, NY, https://hastie.su.domains/ISLR2/ISLRv2_corrected_June_2023.pdf.

Kim, M., Hizir, O., Turan, O., Day, S., Incecik, A., 2017. Estimation of added resistance and ship speed loss in a seaway. Ocean Eng. 141, 465–476. http://dx.doi.org/10.1016/j.oceaneng.2017.06.051, https://linkinghub.elsevier.com/retrieve/pii/S0029801817303530.

Kim, Y.-R., Jung, M., Park, J.-B., 2021. Development of a fuel consumption prediction model based on machine learning using ship in-service data. J. Mar. Sci. Eng. 9 (2), 137. http://dx.doi.org/10.3390/jmse9020137, https://www.mdpi.com/2077-1312/9/2/137.

Kim, Y.-R., Steen, S., Kramel, D., Muri, H., Strømman, A.H., 2023. Modelling of ship resistance and power consumption for the global fleet: The MariTEAM model. Ocean Eng. 281, 114758. http://dx.doi.org/10.1016/j.oceaneng.2023.114758, https://linkinghub.elsevier.com/retrieve/pii/S0029801823011423.

Kumar, R., Carroll, C., Hartikainen, A., Martin, O., 2019. Arviz a unified library for exploratory analysis of Bayesian models in python. J. Open Source Softw. 4 (33), 1143. http://dx.doi.org/10.21105/joss.01143, http://joss.theoj.org/papers/10.21105/joss.01143.

Lang, X., Mao, W., 2020. A semi-empirical model for ship speed loss prediction at head sea and its validation by full-scale measurements. Ocean Eng. 209, 107494. http://dx.doi.org/10.1016/j.oceaneng.2020.107494, https://linkinghub.elsevier.com/retrieve/pii/S0029801820305072.

Lindstad, E., Borgen, H., Eskeland, G.S., Paalson, C., Psaraftis, H., Turan, O., 2019. The need to amend IMO's EEDI to include a threshold for performance in waves (realistic sea conditions) to achieve the desired GHG reductions. Sustainability 11, 3668. http://dx.doi.org/10.3390/su11133668, https://www.mdpi.com/2071-1050/11/13/3668.

Majidian, H., Azarsina, F., 2019. Numerical simulation of container ship in oblique winds to develop a wind resistance model based on statistical data. J. Int. Marit. Saf. Environ. Aff. Shipp. 2 (2), 67–88. http://dx.doi.org/10.1080/25725084.2018.1564471, https://www.tandfonline.com/doi/full/10.1080/25725084.2018.1564471.

Megawati, S., Aisjah, A.S., Widjaja, S., 2023. Prediction of ship fuel consumption due to the effect of weather conditions. In: 2023 International Seminar on Intelligent Technology and Its Applications. ISITIA, IEEE, pp. 786–791. http://dx.doi.org/10.1109/ISITIA59021.2023.10221158, https://ieeexplore.ieee.org/document/10221158/.

Meng, Q., Du, Y., Wang, Y., 2016. Shipping log data based container ship fuel efficiency modeling. Transp. Res. B 83, 207–229. http://dx.doi.org/10.1016/j.trb.2015.11.007.

Panagakos, G., Pessôa, T.d.S., Dessypris, N., Barfod, M.B., Psaraftis, H.N., 2019. Monitoring the carbon footprint of dry bulk shipping in the EU: An early assessment of the MRV regulation. Sustainability 11 (18), 5133. http://dx.doi.org/10.3390/su11185133, https://www.mdpi.com/2071-1050/11/18/5133.

Pedregosa, F., Michel, V., Grisel, O., Blondel, M., Prettenhofer, P., Weiss, R., Vanderplas, J., Cournapeau, D., Pedregosa, F., Varoquaux, G., Gramfort, A., Thirion, B., Grisel, O., Dubourg, V., Passos, A., Brucher, M., Perrot andÉdouardand, M., Duchesnay, a., Duchesnay, É., 2011. Scikit-learn: Machine learning in python. J. Mach. Learn. Res. 12 (85), 2825–2830, http://jmlr.org/papers/v12/pedregosa11a.html.

Perera, L.P., Mo, B., 2018. Ship speed power performance under relative wind profiles in relation to sensor fault detection. J. Ocean Eng. Sci. 3 (4), 355–366. http://dx.doi.org/10.1016/j.joes.2018.11.001, https://linkinghub.elsevier.com/retrieve/pii/S2468013318300950.

Polakis, M., Zachariadis, P., de Kat, J.O., 2019. The energy efficiency design index (EEDI). In: Psaraftis, H.N. (Ed.), Sustainable Shipping. Springer Nature Switzerland, Cham, pp. 93–135. http://dx.doi.org/10.1007/978-3-030-04330-8{_}3, http://link.springer.com/10.1007/978-3-030-04330-8_3.

Psaraftis, H.N., Lagouvardou, S., 2023. Ship speed vs power or fuel consumption: Are laws of physics still valid? Regression analysis pitfalls and misguided policy implications. Clean. Logist. Supply Chain 7, 100111. http://dx.doi.org/10.1016/j.clscn.2023.100111, https://linkinghub.elsevier.com/retrieve/pii/S2772390923000203.

Rehmatulla, N., Parker, S., Smith, T., Stulgis, V., 2017. Wind technologies: Opportunities and barriers to a low carbon shipping industry. Mar. Policy 75, 217–226. http://dx.doi.org/10.1016/j.marpol.2015.12.021, https://linkinghub.elsevier.com/retrieve/pii/S0308597X15003917.

Salvatier, J., Wiecki, T.V., Fonnesbeck, C., 2016. Probabilistic programming in python using PyMC3. PeerJ Comput. Sci. 2 (4), e55. http://dx.doi.org/10.7717/peerj-cs.55, https://peerj.com/articles/cs-55.

Smith, T.W.P., Jalkanen, J.P., Anderson, B.A., Corbett, J.J., Faber, J., Hanayama, S., O'Keeffe, E., Parker, S., Johansson, L., Aldous, L., Raucci, C., Traut, M., Ettinger, S., Nelissen, D., Lee, D.S., Ng, S., Agrawal, A., Winebrake, J.J., Hoen, A., 2014. Third IMO Greenhouse Gas Study 2014. Tech. Rep., International Maritime Organization (IMO), London, UK, p. 327. http://dx.doi.org/10.1007/s10584-013-0912-3.

Tadros, M., Vettor, R., Ventura, M., Guedes Soares, C., 2022. Effect of different speed reduction strategies on ship fuel consumption in realistic weather conditions. In: Trends in Maritime Technology and Engineering Volume 1. CRC Press, London, pp. 553–561. http://dx.doi.org/10.1201/9781003320272-62, https://www.taylorfrancis.com/books/9781003320272/chapters/10.1201/9781003320272-62.

Taskar, B., Regener, P.B., Andersen, P., 2021. The impact of variation in added resistance computations on voyage performance prediction. In: Okada, T., Suzuki, K., Kawamura, Y. (Eds.), Practical Design of Ships and Other Floating Structures. Springer Singapore, pp. 133–149. http://dx.doi.org/10.1007/978-981-15-4624-2{_}8, http://link.springer.com/10.1007/978-981-15-4624-2_8.

The PyMC Development Team, 2023. Pymc.data — PyMC 5.7.1 documentation. https://www.pymc.io/projects/docs/en/stable/api/generated/pymc.Data.html.

Toffoli, A., Bitner-Gregersen, E.M., 2017. Types of ocean surface waves, wave classification. In: Carlton, J., Jukes, P., Choo, Y. (Eds.), Encyclopedia of Maritime and Offshore Engineering. Wiley, Chichester, UK, pp. 1–8. http://dx.doi.org/10.1002/9781118476406.emoe077, https://onlinelibrary.wiley.com/doi/10.1002/9781118476406.emoe077.

Tran, T.A., 2021. Effects of the uncertain factors impacting on the fuel oil consumption of sea ocean-going vessels based on the hybrid multi criteria decision making method. Ocean Eng. 239, 109885. http://dx.doi.org/10.1016/j.oceaneng.2021.109885, https://linkinghub.elsevier.com/retrieve/pii/S0029801821012336.

Vettor, R., Guedes Soares, C., 2022. Reflecting the uncertainties of ensemble weather forecasts on the predictions of ship fuel consumption. Ocean Eng. 250, 111009. http://dx.doi.org/10.1016/j.oceaneng.2022.111009.

Vinayak, P.P., Prabu, C.S.K., Vishwanath, N., Prakash, S.O., 2021. Numerical simulation of ship navigation in rough seas based on ECMWF data. Brodogradnja 72 (1), 19–58. http://dx.doi.org/10.21278/brod72102, https://hrcak.srce.hr/file/368062.

Wang, S., Ji, B., Zhao, J., Liu, W., Xu, T., 2018. Predicting ship fuel consumption based on LASSO regression. Transp. Res. D 65, 817–824. http://dx.doi.org/10.1016/j.trd.2017.09.014.

Wang, S., Psaraftis, H.N., Qi, J., 2021. Paradox of international maritime organization's carbon intensity indicator. Commun. Transp. Res. 1, 100005. http://dx.doi.org/10.1016/J.COMMTR.2021.100005, https://linkinghub.elsevier.com/retrieve/pii/S2772424721000056.

Yan, R., Wang, S., Du, Y., 2020. Development of a two-stage ship fuel consumption prediction and reduction model for a dry bulk ship. Transp. Res. 138 (101930), http://dx.doi.org/10.1016/j.tre.2020.101930.

Zhang, S., Li, Y., Yuan, H., Sun, D., 2019. An alternative benchmarking tool for operational energy efficiency of ships and its policy implications. J. Clean. Prod. 240 (118223), http://dx.doi.org/10.1016/j.jclepro.2019.118223.